Studies on the early physiological responses governing heat stress-inducible gene expression in the red alga *Neopyropia yezoensis*

(スサビノリの高温ストレス誘導性遺伝子発現を司る初期生理応答の研究)

Division of Marine Life Science

Graduate School of Fisheries Sciences

Hokkaido University

北海道大学大学院水産科学院

海洋応用生命科学専攻

Ho Viet Khoa

ほー　びーと　こあ

2022 年

Contents

Abstract

主論文の要約

博士の専攻分野の名称: 博士（水産科学)　　氏名： Ho Viet Khoa

学 位 論 文 題 目

Studies on the early physiological responses governing heat stress-inducible gene expression in the red alga *Neopyropia yezoensis*
(スサビノリの高温ストレス誘導性遺伝子発現を司る初期生理応答の研究)

Heat stress responses are complex regulatory processes, including sensing, signal transduction, and gene expression. However, the exact mechanisms of these processes in seaweeds are not well known. We explored the relationship between membrane physical states and gene expression in the red alga *Neopyropia yezoensis*. To analyze heat stress-induced gene expression, we identified two homologs of the heat-inducible high temperature response 2 (*HTR2*) gene in *Neopyropia seriata*, named *NyHTR2* and *NyHTR2L*. We found conservation of *HTR2* homologs only within the order Bangiales; their products contained a novel conserved cysteine repeat we designated the Bangiales cysteine-rich motif. A quantitative mRNA analysis showed that expression of *NyHTR2* and *NyHTR2L* was induced by heat stress. However, the membrane fluidizer benzyl alcohol (BA) did not induce expression of these genes, indicating that the effect of heat was not

due to membrane fluidization. In contrast, expression of genes encoding multiprotein-bridging factor 1 (*NyMBF1*) and heat shock protein 70 (*NyHSP70-1* and *NyHSP70-2*) was induced by heat stress and by BA, indicating that it involved a membrane fluidization-dependent pathway. In addition, dark treatment under heat stress promoted expression of *NyHTR2*, *NyHTR2L*, *NyMBF1*, and *NyHSP70-2* but not *NyHSP70-1*; expression of *NyHTR2* and *NyHTR2L* was membrane fluidization independent and that of other genes was membrane fluidization dependent. These findings indicate that the heat stress response in *N. yezoensis* involves membrane fluidization-dependent and -independent pathways.

Introduction

Increases in seawater temperature reduce the productivity and quality of economically important red algae of the order Bangiales, such as *Neopyropia yezoensis* and *Neopyropia haitanensis* (Yoshida et al., 2019, Hwang and Park, 2020). Recent comparative transcriptome analyses have demonstrated that these algae respond to heat stress through alteration of gene expression profiles (Sun et al., 2015, Wang et al., 2018), indicating that red algae have heat-inducible genes. Indeed, heat-inducible expression of genes encoding heat shock protein 70 (HSP70) and nuclear localizing high temperature response 2 (HTR2) have been confirmed in *N. yezoensis*, *N. haitanensis*, and *Neopyropia seriata* (Zhou et al., 2011, Kim et al., 2011, Ji et al., 2015, Yu et al., 2021). In addition, the presence of an intrinsic ability to memorize non-lethal heat stress, which enables survival under lethal temperature by establishment of heat stress tolerance, was confirmed in '*Bangia*' sp. ESS1 (Kishimoto et al., 2019); however, other '*Bangia*' species lack this heat stress memory (Khoa et al., 2021). Therefore, elucidation of mechanisms regulating responses to heat stress and procurement of heat stress tolerance based on heat stress memory is indispensable for building strategies to protect the economically important Bangiales from seawater warming.

Responsibility to heat stress with changes in gene expression pattern, morphology and composition of metabolites is evolutionally conserved in green

lineage including terrestrial plants and their closest algal relatives (de Vries et al., 2020, de Vries et al., 2020, Mueller et al., 2015, Ludwig et al., 2021, Rieseberg et al., 2022). However, it seems that there are both conserved and diversified parts in the regulatory mechanisms of these physiological and molecular responses to heat stress among Archaeplastida. In terrestrial plants, heat-inducible transcription of the gene encoding the class A3 heat shock factor (HsfA3), which is a transcription factor regulating mRNA expression of heat shock protein (*HSP*) genes, is controlled by the APETALA2 (AP2) domain transcription factor dehydration-responsive element-binding protein 2A (DREB2A) (Schramm et al., 2008, Yoshida et al., 2008). In addition, expression of DREB2A is heat-inducible through regulation by the class A1 *Hsfs*, such as *HsfA1a*, *HsfA1b*, *HsfA1d*, and *HsfA1e* (Ohama et al., 2017, Yoshida et al., 2011). These findings indicate that the heat stress-inducible expression of *HSP* genes involves a stepwise activation cascade of transcription factors. In fact, genome and extensive transcriptome analyses clearly demonstrated a lack of AP2 domain-containing proteins in red algae, suggesting that the heat signal transduction pathways in Bangiales differ from those in terrestrial plants. Moreover, although the presence of the *HSF* gene was confirmed in Bangiales, including *N. yezoensis* and *Porphyra umbilicalis* (Petroll et al., 2021), as well as in unicellular red algae and Florideophyceae (Petroll et al., 2021, Thiriet-Rupert et al., 2016), little is known about the activation mode and function of *HSF* gene in red algae. Regulatory mechanisms of heat stress

responses in Bangiales remain unknown.

Heat stress increases plant membrane fluidity (Lawal et al., 2017, Rawat et al., 2021). Therefore, homeostasis of the membrane physical state under heat stress is balanced by an increase in saturation level due to accumulation of saturated fatty acids, which increases membrane rigidity and lowers membrane fluidity (Falcone et al., 2004, Higashi et al., 2019, Narayanan, 2020, Shiva et al., 2020, Zoong et al., 2021). Thus, sensing of membrane fluidization is thought to trigger plant heat stress responses (Saidi et al., 2011, Abdelrahman et al., 2020, Hayes et al., 2020, Bourgine et al., 2021). Evidence for this includes an artificial increase in the saturation level of membrane fatty acids following pharmacological treatment with the membrane fluidizer benzyl alcohol (BA) (Sangwan et al., 2010, Königshofer et al., 2008, Finka and Goloubinoff, 2014) and the genetic inactivation of fatty acid desaturase and glycerol-3-phosphate acyltransferase genes in terrestrial plants (Murakami et al., 2000, Yan et al., 2008, Wang et al., 2010). In '*Bangia'* sp. ESS1 (order: Bangiales), a moderate increase in the saturation rate of membrane fatty acids under heat stress conditions promotes acquisition of heat stress tolerance through the establishment of heat stress memory (Kishimoto et al., 2019). However, it is unknown whether heat stress-induced gene expression is initiated by changes in membrane fluidity.

In the present study, we analyzed the relationship between membrane

fluidization and the expression of genes encoding novel cysteine-rich domain proteins (homologs of *HTR2* of *N. seriata* (Kim et al., 2011); *HSP70s* (Zhou et al., 2011), and multiprotein bridging factor 1 (*MBF1* (Uji et al., 2010)) in the red alga *N. yezoensis*. Our findings demonstrate that both membrane fluidization-dependent and -independent pathways regulate heat-inducible gene expression and that these pathways can be enhanced by dark conditions. These findings provide insights into the triggers of heat stress responses in poikilothermic organisms.

Materials and Methods

1. Algal materials and culture conditions

Gametophytes, sporophytes, and conchosporophytes of *N. yezoensis* strain U-51 (Figure 1; Mikami et al., 2019) were maintained in sterilized artificial seawater (SEALIFE, Marinetech, Tokyo, Japan) enriched with ESS2 (Li et al., 2019) under 60–70 μmol photons m^{-2} s^{-1} light with a short-day photoperiod (10 h light/14 h dark) at 15°C with air filtered through a 0.22-μm filter (Whatman, Maidstone, UK). The culture medium was changed weekly.

Three life cycle generations were subjected to temperature stress, which commenced at 12:00, 3 h after the start of light irradiation (9:00). Stress treatment was performed by incubating algae at 5, 15, and 25°C for 0.5, 1, 2, 4, 6, 8, and 12 h. Since the duration of light irradiation was only 10 h, the 8 and 12h incubations included 1 and 5 h of dark conditions, respectively. Experiments were also carried out with 24 h light.

Pharmacological treatment with BA (2.5 mM) and dimethyl sulfoxide (DMSO, 4%) was performed by incubating algae at 15°C for 5, 15, and 30 min. Incubations at 25°C for 8 and 12 h under light with BA or dark conditions with DMSO were also performed. Temperature-stressed and pharmacologically treated gametophytes, sporophytes, and conchosporophytes were harvested, frozen in liquid nitrogen, and stored at -80°C prior to use for gene expression analysis.

2. Identification and phylogenetic analysis of HTR2 homologs

A homology search using our *N. yezoensis* transcriptome data (Mikami et al., 2019) was performed against the *NsHTR2* amino acid sequence to find candidate *NsHTR2* homologs. The ORF finder (https://www.ncbi.nlm.nih.gov/orffinder/) was used to identify full-length open reading frames (ORFs) of these candidates. A BLAST search (https://blast.ncbi.nlm.nih.gov/Blast.cgi) using predicted amino acid sequences of *NsHTR2* and candidates from *N. yezoensis* as queries was performed to find HTR2 homologs from other algae and terrestrial plants. The amino acid sequences of all the obtained HTR2 homologs were used to construct a neighbor-joining phylogenetic tree with MEGA 7 (https://www.megasoftware.net) using ClustalW to align the sequences. The accession numbers of the sequences, except for *NsHTR2*, from DDBJ/EMBL/GenBank are shown next to the species names in the phylogenetic tree in Figure 2.

3. Total RNA extraction and cDNA synthesis

Extraction of total RNA from gametophytes, sporophytes, and conchosporophytes, removal of genomic DNA contamination, quality check of purified total RNA, and synthesis of first-strand complementary DNA (cDNA) were performed as describing in Li et al. (2019). The thermal cycling parameters

for the first-strand cDNA synthesis consisted of an initial denaturation step at 98°C for 30 s; 30 cycles of 98°C for 10 s, 60°C for 30 s, and 72°C for 20 s; and a final extension step at 72°C for 5 min.

4. Quantitative gene expression analysis

Primers for quantitative PCR were designed using Primer Premier 5 (http://www.premierbiosoft.com) and confirmed productivity of PCR products with expected sizes according to Li et al. (2019). We used two real-time PCR (RT-PCR) machines. The thermal cycling parameters for the Applied Biosystems 7300 RT-PCR system (Life Technologies, Carlsbad, USA) consisted of 95°C for 5 min and 40 cycles of 94°C for 30 s, 60°C for 30 s, and 72°C for 20 s. The thermal cycling parameters for the AriaMX (3000P) real-time PCR system (Agilent Technologies, California, USA) consisted of 95°C for 3 min and 40 cycles of 95°C for 5 s and 60°C for 20 s. A dissociation curve was generated to check for specificity of amplification by heating from 60 to 95°C in the Applied Biosystems 7300 RT-PCR system or by 95°C for 1 min, 55°C for 30 s, and 95°C for 30 s in the AriaMX (3000P) real-time PCR system.

5. Statistical analysis

Values are presented as the mean ± SD from triplicate experiments. One

way and two way ANOVA followed by a *Tukey-Kramer* test was used for multiple comparisons, and significant differences were determined using a cutoff value of $p < 0.05$.

Results

1. Determination of a reference gene for quantitative analysis of heat-inducible gene expression

We selected three candidate reference genes for quantitative RT-PCR (qRT-PCR) analysis of heat-inducible gene expression in three generations of the *N. yezoensis* life cycle, i.e., gametophyte, sporophyte, and conchosporophyte: *GAPDH* (glyceraldehyde 3-phosphate dehydrogenase), *EF1α* (Elongation factor1-α), and *eIF4A* (Translation initiation factor 4A). These were previously proposed as reference genes for qRT-PCR in *N. yezoensis* (Wu et al., 2013, Kong et al., 2015). We validated the specificity and efficiency of the newly designed primer pairs (Table 1) by 2% agarose gel electrophoresis of amplicons of each candidate gene derived from cDNA libraries of gametophytes, sporophytes, and conchosporophytes. A single PCR fragment with expected size was amplified, which gave rise to a single peak in the melting curve (data not shown). The amplification efficiency (E) of each set ranged from 95.13 to 102.55%, and the linear correlation coefficients (R^2) ranged from 0.9948 to 0.9973 (Table 1), both of which were within the acceptable range (E: 90-105%; R2: 0.9910-0.9998). Moreover, we were able to generate standard curves for all primer sets using a 10-fold dilution series with six dilution points in triplication (data not shown). Thus, all primer sets are suitable for further characterization of candidates as desired

reference genes.

We calculated the expression stability of these candidates by measuring the cycle threshold (Ct) values of the genes. We synthesized template cDNAs for qRT-PCR using total RNAs separately prepared from three generations, each of which were a mixture of one control sample and triplicate samples treated with 5, 15, or 25°C for 0.5, 1, 2, 4, 6, 8, or 12 h for each generation (a total of 22 samples for each generation). The Ct values of reference genes ranged from 17.4 to 23.8, 16.7 to 23.2, and 18.3 to 24.3 in gametophytes, sporophytes, and conchosporophytes, respectively (Figure 4A). Of the candidates, *EF1α* displayed the lowest expression level, while both *GAPDH* and *eIF4A* had the highest expression levels (Figure 4A). Next, we used geNorm software to rank the expression stability of each gene by calculating the expression stability value. Figure 4B shows the average expression stability M of three candidates. *eIF4A* was the most stable, with M < 1.5 in all of generations. Moreover, *eIF4A* was ranked as the most stable gene in all three life cycle generations using NormFinder (Table 2). Therefore, we concluded that *eIF4A* is a suitable reference gene for normalizing gene expression under both heat and cold stress conditions in all life cycle generations.

To confirm the above findings, we subjected all the candidate reference genes to qRT-PCR to examine *NyMBF1* expression across *N. yezoensis* generations under heat (25°C) and cold (5°C) stress (see Table 3 for primers). Our

rationale was that it seemed plausible that *NyMBF1* expression might be induced by heat stress, as occurs with numerous genes in terrestrial plants (Jaimes-Miranda et al., 2020). We incubated algae from each of the three generations separately at 5, 15, or 25°C for 0.5, 1, 2, 4, 6, 8, or 12 h. When we normalized qRT-PCR data using *eIF4A* as the reference gene, it was clear that heat (but not cold) induced the expression of *NyMBF1* in all three generations, with peaks at 2 and 8 h after exposure to 25°C. In contrast, when we normalized the data using *GAPDH* or *EF1α*, we did not observe heat-dependent expression of *NyMBF1* (Figures 5-7, Table 4). These findings indicate that *NyMBF1* is a heat stress-inducible gene, and *eIF4A* is a suitable reference gene to use in monitoring gene expression under heat and cold stress in the three generations of *N. yezoensis*. Accordingly, we employed *eIF4A* as a reference gene in the rest of our study.

2. Heat-inducible and dark-stimulated expression of high temperature response genes

2.1 Discovery of a novel protein family specifically conserved in Bangiales

By homology searching of the transcriptome data of *N. yezoensis* (Mikami et al., 2019), we found two homologs (Unigene16775 and CL1219.Contig1) of *NsHTR2*, which has been identified as a heat-inducible gene in *N. seriata* (Kim et al., 2011). In addition, we identified eight homologs (OSX78858, OSX74332,

OSX76372, OSX71170, OSX80752, OSZ76191, OSX79754, and OSX68660) from the red alga *P. umbilicalis* (Brawley et al., 2017) through an NCBI BLAST search with *NsHTR2* as a query. We found no other homologs among florideophyceans, green and brown algae, or terrestrial plants, indicating that HTR2 is a Bangiales-specific protein. Phylogenetic analysis using amino acid sequences of the proteins revealed two clades (Figure 2): an HTR2 clade containing all *Neopyropia* proteins and five *P. umbilicalis* proteins (OSX78858, OSX74332, OSX76372, OSX71170, and OSX80752) and a clade of HTR2-related proteins that contains OSZ76191, OSX79754, and OSX68660 from *P. umbilicalis*. Since Unigene16775 is more closely related to *NsHTR2* than to CL1219.Contig1, we designated Unigene16775 and CL1219.Contig1 as *NyHTR2* and *NyHTR2L* (HTR2 like), respectively. The DDBJ/EMBL/GenBank accession numbers of *NyHTR2* and *NyHTR2L* are LC672062 and LC672063, respectively. It is unknown whether *N. seriata* has other HTR2 homologs.

Amino acid alignment indicated that all the HTR2 homologs have a unique domain at their C-terminal half in which the positions of 10 cysteine (Cys) residues were highly conserved (Figure 3). Cross-brace zinc finger motifs, such as RING, PHD, FYVE, and ZZ fingers, are structural features that bind zinc atoms through eight Cys and/or His ligands, each with a specific biological role (Miyamoto et al., 2017, Miyamoto et al., 2019). However, the Cys-rich domains of the HTR2 proteins differed from previously identified cross-brace zinc fingers and did not

show sequence similarity to any conserved domains based on three-dimensional structure predictions with the Phyre2 Server (http://www.sbg.bio.ic.ac.uk/phyre2/html/). Thus, HTR2 homologs are novel proteins containing an unknown Cys-repeat motif. Since it is uncertain whether this motif is a new type of cross-brace zinc finger, we designated it the Bangiales cysteine-rich (BCR) motif.

2.2 Heat-inducible and dark-stimulated expression of high temperature response genes

Since HTR2 has been identified as a heat-inducible gene in *N. seriata* (Kim et al., 2011), we analyzed expression profiles of both *NyHTR2* and *NyHTR2L* under the same cold and heat stress conditions as those used to analyze *NyMBF1* (Figures 5-7, Table 4) using primers showed in Table 3. *NyHTR2* was expressed only in gametophytes and was induced by heat stress (Figure 8, Table 5). *NyHTR2* expression peaked at 2 and 8 h after exposure to 25°C (Figure 8, Table 5). Since *N. yezoensis* was cultured under a short-day photoperiod (10 h light:14 h dark) and the temperature treatments began 3 h into the light period, the *NyHTR2* expression peak at 8 h occurred 1 h after the start of the dark period. Therefore, the first and second *NyHTR2* expression peaks occurred under heat and heat plus dark conditions, respectively. Moreover, *NyHTR2L* was induced by heat stress in all three generations, with expression peaks at 2 and 8 h after exposure to 25°C heat

stress (Figure 8). *NyMBF1* expression followed the same pattern in all three generations (Figures 5-7, Table 4). Therefore, the heat-inducible expression patterns of *NyHTR2*, *NyHTR2L*, and *NyMBF1* were identical, although temporal expression patterns of *NyHTR2* during the life cycle differed from those of other genes.

We also reexamined the heat-inducible expression of *NyHSP70-1* and *NyHSP70-2* (see Table 3 for primers), which had been demonstrated previously (Zhou et al., 2011). In gametophytes, both genes had expression peaks at 2 h after heat exposure. *NyHSP70-2*, but not *NyHSP70-1*, also showed a second peak at 8 h after exposure (Figure 9, Table 6). We observed similar expression patterns in sporophytes and conchosporophytes. Expression peaks in conchosporophytes occurred rapidly, at 1 h after exposure (Figure 9, Table 6). These findings indicate that the appearance of a second expression peak under heat plus dark conditions varies depending on the gene.

To further explore the drivers of the second expression peak, we changed the culture conditions to 24 h light. Under these conditions, we did not observe a second expression peak for *NyHTR2*, *NyHTR2L*, *NyMBF1*, or *NyHSP70-2* in any generation (8L and 12L in Figures 10 and 11). There was no expression peak for *NyHSP70-1* under either regular or 24 h light conditions (Figures 10 and 11). These findings indicate that the second expression peak requires darkness as well as heat

stress. Thus, dark conditions result in a second, heat stress-dependent induction of *NyHTR2*, *NyHTR2L*, *NyMBF1*, and *NyHSP70-2* expression after the first transient expression, which is inhibited by light illumination.

3. Relationship between heat-inducible expression and membrane fluidization

Membrane fluidization caused by heat stress triggers heat induced gene expression in terrestrial plants (Saidi et al., 2011, Abdelrahman et al., 2020, Bourgine et al., 2021, Hayes et al., 2020); however, it is unknown whether changes in membrane physical state are related to gene expression in seaweeds. Thus, we examined the effects of a membrane fluidizer, benzyl alcohol (BA), and a membrane rigidizer, (DMSO), on the expression of heat-inducible genes.

Treatment with 2.5 mM BA at 15°C did not induce expression of *NyHTR2* or *NyHTR2L* but did (like heat stress) induce expression of *NyMBF1*, *NyHSP70-1*, and *NyHSP70-2* (Figures 12 and 13). In contrast, treatment with 4% DMSO did not induce expression of *NyHTR2*, *NyHTR2L*, *NyMBF1*, or *NyHSP70-2* but did induce expression of *NyHSP70-1* (Figures 12 and 13). This indicates that the heat-induced expression of *NyHTR2* or *NyHTR2L* is not dependent on membrane fluidization, whereas that of *NyMBF1*, *NyHSP70-1*, and *NyHSP70-2* is fluidization dependent.

Both cold stress and DMSO rigidify membranes; however, a 5°C exposure did not induce expression of *NyHSP70-1* (Figure 9). To further assess whether *NyHSP70-1* responds to low temperatures, we examined the expression of *NyHSP70-1* and other genes in algae exposed to a temperature of 0°C. Only *NyHSP70-1* was induced by 0°C treatment (Figure 14). Thus, *NyHSP70-1* is inducible by both heat and cold, whereas the other genes we examined were only inducible by heat.

Finally, we performed two experiments to confirm whether membrane fluidization is required for the second peak seen under dark conditions. First, we subjected the three generations of algae to 25°C and 2.5 mM BA under continuous light. This treatment induced the expression of *NyHSP70-1* and *NyHSP70-2*, as detected 1 h after BA application, but had no effect on the expression of *NyHTR2* or *NyHTR2L* (Figure 15). BA application also induced *NyMBF1* in gametophytes but not in conchosporophytes (Figure 16). In the second experiment, we subjected the three generations of algae to heat stress, either with or without 4% DMSO, under dark conditions. In gametophytes, DMSO reduced expression levels of all genes except *NyHSP70-1* (Figure 16). This is consistent with our earlier results regarding the effect of DMSO treatment on *NyHSP70-1* under dark conditions (Figures 9 and 11). Therefore, there are at least two signal transduction pathways regulating the second expression peak under dark conditions at 25°C: a pathway involving dark-dependent membrane fluidization that governs *NyMBF1* and

NyHSP70-2 expression and another pathway that, though heat dependent, does not involve membrane fluidization and that governs *NyHTR2* and *NyHTR2L* expression.

Discussion

In the present study, we examined the involvement of membrane fluidity in heat stress-inducible gene expression in the red alga *N. yezoensis*. We identified two genes encoding *NsHTR2* homologs in *N. yezoensis*, which we designated *NyHTR2* and *NyHTR2L* (Figure 2). The *NsHTR2* homologs contained a novel Cys-repeat motif that was conserved only in Bangiales and which we therefore designated the Bangiales Cys-repeat (BCR) motif. We identified *NyHTR2* as a gametophyte-specific gene (Figure 4). Both *NyHTR2* and *NyHTR2L* were heat stress-inducible but did not depend on the membrane fluidization that generally results from heat stress, as evidenced by their lack of induction by the membrane fluidizer BA (Figures 12 and 14). In contrast, expression of *NyMBF1*, *NyHSP70-1*, and *NyHSP70-2* was induced not only by heat but also by membrane fluidization (BA treatment); thus, we consider them to be membrane fluidization dependent (Figures 14 and 16). Therefore, we conclude that *N. yezoensis* has both membrane fluidization-dependent and -independent pathways of heat-inducible expression.

We found that dark conditions stimulated both the membrane fluidization-dependent and -independent pathways, but in different fashions. The heat-inducible genes had an initial, transient low-level expression peak at 4-6 h after heat exposure in the light (Figures 5-9). A second expression peak occurred 1 h after the dark period began; however, this did not occur when *N. yezoensis* was

grown under continual light at 25°C (Figures 10 and 11). This indicates that the three generations of *N. yezoensis* could tolerate continual heat stress after the first peak; however, dark exposure reset the heat stress response and resulted in a second expression peak. Moreover, it is likely that membrane fluidization is involved in the second heat-induced expression peak of *NyMBF1* and *NyHSP70-2* because BA treatment also induced a second expression peak of these genes under continual light, whereas DMSO reduced the second expression peak in the dark period (Figures 12 and 13).

In contrast, the second, dark-induced expression peaks of *NyHTR2* and *NyHTR2L* were not sensitive to BA application, indicating that they are independent of membrane fluidization. However, DMSO treatment reduced the dark-induced expression of these genes (Figure 13). DMSO is a membrane rigidizer and is often used to study physiological responses to membrane rigidification, such as cold stress-inducible gene expression (Sangwan et al., 2010, Suri et al., 2008). Therefore, the fact that DMSO reduced *NyHTR2* and *NyHTR2L* expression is inconsistent with the BA treatment results. In the unicellular green alga *Chlamydomonas reinhardtii*, transcripts of HSF1, HSP70A, HSP90A, and HSP90C accumulated under treatment with heat plus DMSO, an effect similar to that of the cytosolic translation inhibitor cycloheximide. Therefore, DMSO-dependent translational inhibition is proposed to be responsible for the enhanced expression of these genes caused by DMSO (Schmollinger et al., 2013, Rütgers et

al., 2017). It is possible that translational inhibition by DMSO is also related to *NyHTR2* and *NyHTR2L* expression; however, this remains to be confirmed.

On the basis of our findings, we conclude that there are multiple pathways regulating heat stress-inducible gene expression in *N. yezoensis*. One is a membrane fluidization-dependent pathway, which can be subdivided into a dark-enhanced pathway for *NyMBF1* and *NyHSP70-2* and a dark-independent pathway for *NyHSP70-1*. Similarly, moss membrane proteins, including the cyclic nucleotide-gated Ca^{2+} channels CNGCb and CNGCd, are membrane fluidization-dependent heat-sensing molecules (Zoong et al., 2021, Finka and Goloubinoff, 2014, Saidi et al., 2009). Therefore, it could be valuable to explore the involvement of Ca^{2+} influx and cyclic nucleotide-gated Ca^{2+} channels in early heat stress responses in *N. yezoensis*. The other pathway regulating heat stress-inducible gene expression in *N. yezoensis* is a membrane fluidization-independent pathway directing *NyHTR2* and *NyHTR2L* expression, which is enhanced by dark conditions. The discovery of this pathway was unexpected because heat stress responses are generally thought to be triggered by membrane fluidization (Saidi et al., 2009, Abdelrahman et al., 2020, Hayes et al., 2020, Bourgine et al., 2021, Cano-Ramirez et al., 2021). Thus, further examination of heat stress-inducible expression of *NyHTR2* and *NyHTR2L* might uncover novel mechanisms of heat stress responses in photosynthetic organisms.

Alone among the genes examined in this study, *NyHSP70-1* was induced by both DMSO treatment and cold stress (Figures 13 and 16), indicating that it is triggered by cold stress-induced membrane rigidification. Similar cold stress-inducible expression of HSP genes has been reported in various plant species (Anderson et al., 1994, Sabehat et al., 1998, Li et al., 1999, Lopes-Caitar et al., 2013, Deng et al., 2018, Li et al., 2019, Hunter et al., 2021). In our study, *NyHSP70-1* expression was also induced by heat stress and was membrane fluidization dependent, but it was not affected by dark (Figures 9, 11, 13-15). *NyHSP70-1* is therefore an ideal model in which to investigate the regulatory mechanisms of heat and cold stress-inducible gene expression based on physical changes in membranes in Bangiales.

Extracellular Ca^{2+} influxes and reactive oxygen species (ROS) are involved in the early phases of heat stress responses in terrestrial plants (Volkov et al., 2006, Fedyaeva et al., 2014, Awasthi et al., 2015, Sun et al., 2016 Katano et al., 2018). These can be triggered by membrane fluidization (Sangwan et al., 2010, Königshofer et al., 2008, Finka and Goloubinoff , 2014, Saidi et al., 2009, Jajic et al., 2015). However, little is known about how these signaling molecules may be involved in either of the heat stress-induced gene expression pathways in *N. yezoensis*. Therefore, further examination of the membrane fluidization-dependent and -independent pathways could provide novel insights into stress perception and early events in heat stress-inducible gene expression in Bangiales.

Acknowledgments

I would like to give my deepest gratitude to Prof. Koji Mikami, who was belonging to Faculty of Fisheries Sciences, Hokkaido University (Hakodate, Hokkaido), and then Department of Integrative Studies of Plant and Animal Production, School of Food Industrial Sciences, Miyagi University (Sendai, Miyagi), for his great efforts for obtaining a scholarship to stay and study in Japan and his devoted supervision, scholastic guidance, advice and support for my study during the doctoral course.

I appreciate Prof. Hiroyuki Mizuta (Faculty of Fisheries Sciences, Hokkaido University) for permission to study in the Miyagi University with helpful supports and guidance and also Profs. Hideki Kishimura and Masashi Hosokawa (Faculty of Fisheries Sciences, Hokkaido University) for their valuable advice and constructive criticism to improve this thesis with Prof. Mizuta. I acknowledge Prof. Motoko Morimoto (Miyagi University) for technical guidance and support on using a real-time PCR system and making standard curves for quantitative gene expression analysis. I also thank Dr. Puja Kumari, Dr. Chengze Li and Mr. Ryunosuke Irie for their valuable guidance throughout my studies, Dr. Huynh Huu Tho for guidelines for using SPSS software, and all the students in Prof. Mikami's laboratory in Hakodate and Sendai from 2019 to 2022 for their constant spiritual and technical support throughout my whole Ph.D. study.

I acknowledge the Japan Ministry of Education, Culture, Sports, Science and Technology (MEXT) for providing scholarship to study at Hokkaido University and Miyagi University during the Ph.D. course as well as to People's committee of Ca Mau province and People's committee of Dam Doi district (Viet Nam) for acceptation to study in Japan.

I also express the deepest gratefulness to my parents, the family of my two brothers, the family of my sister, for their encouragement, continuous support, wise counsel and sympathetic ear. In particular, I thank the family of Mr. Takahashi Atsushi for their daily support during the period I studied in Sendai, Japan.

References

Abdelrahman, M. L., Ishii, T., El-Sayed, M., Tran, L. S. P. 2020. Heat sensing and lipid reprograming as a signaling switch for heat stress responses in wheat. *Plant Cell Physiol*. 61, 1399-1407.

Anderson, J. V., Li, Q. B., Haskell, D. W., Guy, C. L. 1994. Structural organization of the spinach endoplasmic reticulum-luminal 70-kilodalton heat-shock cognate gene and expression of 70-kilodalton heat-shock genes during cold acclimation. *Plant Physiol*. 104, 1359.

Awasthi, R., Bhandari, K., Nayyar, H. 2015. Temperature stress and redox homeostasis in agricultural crops. *Front. Environ. Sci.* 3, 11.

Bourgine, B., Guihur, A. 2021. Heat shock signaling in land plants: From plasma membrane sensing to the transcription of small heat shock proteins. *Front. Plant Sci*. 12, 710801.

Brawley, S.,H., Blouin, N.,A., Ficko-Blean, E., Wheeler, G.,L., Lohr, M., Goodson, H.,V., Jenkins, J.,W., Blaby-Haas, C.,E., Helliwell, K.,E., Chan, C.,X., Marriage, T.,N., Bhattacharya, D., Klein, A.,S., Badis, Y. Brodie, J. Cao, Y. Collén, J., Dittami, S. M., Gachon, C., Green, B. R., Prochnik, S. E. 2017. Insights into the red algae and eukaryotic evolution from the genome of *Porphyra umbilicalis* (Bangiophyceae, Rhodophyta). *Proc. Natl. Acad. Sci. U.S.A.* 114(31), E6361–E6370.

Cano-Ramirez, D. L., Carmona-Salazar, L., Morales-Cedillo, F., Ramírez-

Salcedo, J., Cahoon, E. B., Gavilanes-Ruíz, M. 2021. Plasma membrane fluidity: An environment thermal detector in Plants. *Cells* 10, 2778.

de Vries, J., de Vries, S., Curtis, B. A., Zhou, H., Penny, S., Feussner, K., Pinto, D. M., Steinert, M., Cohen, A. M., von Schwartzenberg, K., Archibald, J. M. 2020. Heat stress response in the closest algal relatives of land plants reveals conserved stress signaling circuits. *The Plant journal: for cell and molecular biology* 103(3), 1025–1048.

de Vries, J., Ischebeck, T. 2020. Ties between Stress and Lipid Droplets Pre-date Seeds. *Trends Plant Sci.* 25(12), 1203–1214.

Deng, X., Wang, J., Li, Y., Wu, S., Yang, S., Chao, J., Chen, Y., Zhang, S., Shi, M., Tian, W. M. 2018. Comparative transcriptome analysis reveals phytohormone signalings, heat shock module and ROS scavenger mediate the cold-tolerance of rubber tree. *Sci. Rep.* 8, 4931.

Falcone, D. L., Ogas, J. P., Somerville, C. R. 2004. Regulation of membrane fatty acid composition by temperature in mutants of *Arabidopsis* with alterations in membrane lipid composition. *BMC Plant Biol.* 4, 17.

Fedyaeva, A. V., Stepanov, A. V., Lyubushkina, I. V., Pobezhimova, T. P., Rikhvanov, E. G. 2014. Heat shock induces production of reactive oxygen species and increases inner mitochondrial membrane potential in winter wheat cells. *Biochem. (Moscow)* 79, 1202-1210.

Finka, A., Goloubinoff, P. 2014. The CNGCb and CNGCd genes from *Physcomitrella patens* moss encode for thermosensory calcium channels

responding to fluidity changes in the plasma membrane. *Cell Stress Chaperones* 19, 83-90.

Hayes, S., Schachtschabel, J., Mishkind, M., Munnik, T., Arisz, S. A. 2020. Hot topic: Thermosensing in plants. *Plant Cell Environ.* 44, 2018-2033.

Higashi, Y., Saito, K. 2019. Lipidomic studies of membrane glycerolipids in plant leaves under heat stress. *Prog. Lipid Res.* 75, 100990.

Hunter, D. A., Napier, N. J., Erridge, Z. A., Saei, A., Chen, R. K. Y., McKenzie, M. J., O'Donoghue, E. M., Hunt, M., Favre, L., Lill, R. E., Brummell, D. A. 2021. Transcriptome responses of ripe cherry tomato fruit exposed to chilling and rewarming identify reversible and irreversible gene expression changes. *Front. Plant Sci.* 12, 685416.

Hwang, E. K., Park, C. S. 2020. Seaweed cultivation and utilization of Korea. *Algae* 35, 107-121.

Jaimes-Miranda, F., Chávez Montes, R. A. 2020. The plant MBF1 protein family: a bridge between stress and transcription. *J. Exp. Bot.* 71, 1782-1791.

Jajic, I., Sarna, T., Szewczyk, G., Strzalka, K. 2015. Changes in production of reactive oxygen species in illuminated thylakoids isolated during development and senescence of barley. *J. Plant Physiol.* 184, 49-56.

Ji, D., Li, B., Xu, Y., Chen, C., Xie, C. 2015. Cloning and quantitative analysis of five heat shock protein 70 genes from *Pyropia haitanensis*. *J. Appl. Phycol.* 27, 499- 509.

Katano, K., Kataoka, R., Fujii, M., Suzuki, N. 2018. Differences between seedlings and flowers in anti-ROS based heat responses of Arabidopsis plants deficient in cyclic nucleotide gated channel 2. *Plant Physiol. Biochem. 123*, 288-296.

Khoa, H. V., Kumari, P., Uchida, H., Murakami, A., Shimada, S., Mikami, K. 2021. Heat-stress responses differ among species from different *'Bangia'* clades of Bangiales (Rhodophyta). *Plants (Basel)* 22, 1733.

Kim, E., Park, H. S., Jung, Y., Choi, D. W., Jeong, W. J., Park, H. S. 2011. Identification of the high-temperature response genes from *Porphyra seriata* (*Rhodophyta*) expression sequence tags and enhancement of heat tolerance of *Chlamydomonas* (*Chlorophyta*) by expression of the *Porphyra* HTR2 gene1: high-temperature stress in *Porphyra*. *J. Phycol.* 47, 821-828.

Kishimoto, I., Ariga, I., Itabashi, Y., Mikami, K. 2019. Heat-stress memory is responsible for acquired thermotolerance in *Bangia fuscopurpurea*. *J Phycol.* 55, 971-975.

Kong, F., Cao, M., Sun, P., Liu, W., Mao, Y. 2015. Selection of reference genes for gene expression normalization in *Pyropia yezoensis*, using quantitative real-time PCR. *J. Appl. Phycol*. 27, 1003-1010.

Königshofer, H., Tromballa, H. W., Löppert, H. G. 2008. Early events in signaling high- temperature stress in tobacco BY2 cells involve alterations in membrane fluidity and enhanced hydrogen peroxide production. *Plant Cell Environ*. 31, 1771–1780.

Lawal, G., Mohd, S. M. A., Siti, N. O., Raja, N. Z. 2017. Review on fatty acid desaturases and their roles in temperature acclimatisation. *J. Appl. Sci*. 17, 282-295.

Li, C., Ariga, I., Mikami, K. 2019. Difference in nitrogen starvation-inducible expression patterns among phylogenetically diverse ammonium transporter genes in the red seaweed *Pyropia yezoensis*. *Am. J. Plant Sci.* 10, 1325–1349.

Li, Q. B., Haskell, D. W., Guy, C. L. 1999. Coordinate and non-coordinate expression of the stress 70 family and other molecular chaperones at high and low temperature in spinach and tomato. *Plant Mol. Biol.* 39, 21-34.

Lopes-Caitar, V. S., de Carvalho, M. C., Darben, L. M., Kuwahara, M. K., Nepomuceno, A. L., Dias, W. P. 2013. Genome-wide analysis of the Hsp 20 gene family in soybean: Comprehensive sequence, genomic organization and expression profile analysis under abiotic and biotic stresses. *BMC Genomics* 14, 577.

Ludwig, W., Hayes, S., Trenner, J., Delker, C., Quint., M. 2021. On the evolution of plant thermomorphogenesis. *J. Exp. Bot.* 72(21), 7345–7358.

Mikami, K., Li, C., Irie, R. 2019. A unique life cycle transition in the red seaweed *Pyropia yezoensis* depends on apospory. *Commun Biol.* 2, 299.

Miyamoto, K., Fujiwara, Y., Saito, K. 2019. Zinc finger domain of the human DTX protein adopts a unique RING fold. *Protein Sci.* 28, 1151–1156.

Miyamoto, K., Uechi, A., Saito, K. 2017. The zinc finger domain of RING finger protein 141 reveals a unique RING fold. *Protein Sci.* 26, 1681-1686.

Mueller, S.P.; Krause, D.M.; Mueller, M.J.; Fekete, A. 2015. Accumulation of extra-chloroplastic triacylglycerols in Arabidopsis seedlings during heat acclimation. *J. Exp. Bot.* 66(15), 4517–4526.

Murakami, Y., Tsuyama, M., Kobayashi, Y., Kodama, H., Iba, K. 2000. Trienoic fatty acids and plant tolerance of high temperature. *Science* 287, 476-479.

Narayanan, S. 2020. Comparative lipidomic analysis reveals heat stress responses of two soybean genotypes differing in temperature sensitivity. *Plants* 9, 57.

Ohama, N., Sato, H., Shinozaki, K., Yamaguchi-Shinozaki, K. 2017. Transcriptional regulatory network of plant heat stress response. *Trends Plant Sci.* 22, 53-65.

Petroll, R., Schreiber, M., Finke, H., Cock, J. M., Gould, S. B., Rensing, S. A. 2021. Signatures of transcription factor evolution and the secondary gain of red algae complexity. *Genes* 12, 1055.

Rawat, N., Singla-Pareek, S. L., Pareek, A. 2021. Membrane dynamics during individual and combined abiotic stresses in plants and tools to study the same. *Physiol. Plant.* 171, 653-676.

Rieseberg, T. P., Dadras, A., Fürst-Jansen, J., Dhabalia Ashok, A., Darienko, T., de Vries, S., Irisarri, I., de Vries, J. 2022. Crossroads in the evolution of plant specialized metabolism. *Seminars in cell & developmental biology* S1084-9521(22)00073-8.

Rütgers, M., Muranaka, L. S., Schulz- Raffelt, M., Thoms, S., Schurig, J., Willmund, F., Schroda, M. 2017. Not changes in membrane fluidity but proteotoxic stress triggers heat shock protein expression in *Chlamydomonas reinhardtii*. *Plant Cell Environ*. 40, 2987–3001.

Sabehat, A., Lurie, S., Weiss, D. 1998. Expression of small heat-shock proteins at low temperatures. *Plant Physiol.* 117, 651-658.

Saidi, Y., Finka, A, Muriset, M., Bromberg, Z., Weiss, Y.G., Maathuis, F. J., and Goloubinoff, P. 2009. The heat shock response in moss plants is regulated by specific calcium-permeable channels in the plasma membrane. *Plant Cell.* 21, 2829–2843.

Saidi, Y., Finka, A., Goloubinoff, P. 2011. Heat perception and signaling in plants: a tortuous path to thermotolerance. *New Phytol.* 190, 556-65.

Sangwan, V., Orvar, B. L., Beyerly, J., Hirt, H., Dhindsa, R.S. 2010. Opposite changes in membrane fluidity mimic cold and heat stress activation of distinct plant MAP kinase pathways. *Plant J*. 31, 629–638.

Schmollinger, S., Schulz-Raffelt, M., Strenkert, D., Veyel, D., Vallon, O., Schroda, M. 2013. Dissecting the heat stress response in *Chlamydomonas* by pharmaceutical and RNAi approaches reveals conserved and novel aspects. *Mol. Plant* 6, 1795–1813.

Schramm, F., Larkindale, J., Kiehlmann, E., Ganguli, A., Englich, G., Vierling, E., von Koskull-Döring, P.A. 2008. Cascade of transcription factor DREB2A and heat stress transcription factor HsfA3 regulates the heat stress response

of *Arabidopsis*. *Plant J.* 53, 264-74.

Shiva, S. 2020. Leaf lipid alterations in response to heat stress of *Arabidopsis thaliana*. *Plants* 9, 845.

Sun, A. Z., Guo, F. Q. 2016. Chloroplast retrograde regulation of heat stress responses in plants. *Front. Plant Sci. 7*, 398.

Sun, P., Mao, Y., Li, G., Cao, M., Kong, F., Wang, L., Bi, G. 2015. Comparative transcriptome profiling of *Pyropia yezoensis* (Ueda) M.S. Hwang & H.G. Choi in response to temperature stresses. *BMC Genomics* 16, 463.

Suri, S. S., Dhindsa, R. S. 2008. A heat-activated MAP kinase (HAMK) as a mediator of heat shock response in tobacco cells. *Plant Cell Environ.* 31, 218-26.

Thiriet-Rupert, S., Carrier, G., Chénais, B., Trottier, C., Bougaran, G., Cadoret, J. P., Schoefs, B., Saint-Jean, B. 2016. Transcription factors in microalgae: genome-wide prediction and comparative analysis. *BMC Genomics* 17, 282.

Uji, T., Takahashi, M., Saga, N., Mikami, K. 2010. Visualization of nuclear localization of transcription factors with cyan and green fluorescent proteins in the red alga *Porphyra yezoensis*. *Mar. Biotechnol.* 12, 150-159.

Volkov, R. A., Panchuk, I. I., Mullineaux, P. M., Schoffl, F. 2006. Heat stress-induced H_2O_2 is required for effective expression of heat shock genes in *Arabidopsis*. *Plant Mol. Biol.* 61, 733-746.

Wang, H. S., Yu, C., Tang, X. F., Wang, L. Y., Dong, X. C., Meng, Q. W. 2010.

Antisense-mediated depletion of tomato endoplasmic reticulum omega-3 fatty acid desaturase enhances thermal tolerance. *J Integr Plant Biol.* 52(6):568-77.

Wang, W., Teng, F., Lin, Y., Ji, D., Xu, Y., Chen, C. 2018. Transcriptomic study to understand thermal adaptation in a high temperature-tolerant strain of *Pyropia haitanensis*. *PLoS One* 13, e0195842.

Wu, X., Huang, A., Xu, M., Wang, C., Jia, Z., Wang, G., Niu, J. 2013. Variation of expression levels of seven housekeeping genes at different life-history stages in *Porphyra yezoensis*. *PLoS One* 8, e60740.

Yan, K., Chen, N., Qu, Y. Y., Dong, X. C., Meng, Q. W., Zhao, S. J. 2008. Overexpression of sweet pepper glycerol-3-phosphate acyltransferase gene enhanced thermotolerance of photosynthetic apparatus in transgenic tobacco. *J. Integr. Plant Biol*. 50, 613-21.

Yoshida, G., Shimabukuro, H., Kiyomoto, S., Kadota, T., Yoshimura, T., Murase, N., Noda, M., Takenaka, S., Kono, Y., Tamura, T., Tanada, N., Yu, X., Yoshie, N., Guo, X. 2019. Assessment and future prediction of climate change impacts on the macroalgal bed ecosystem and cultivation in the Seto Inland Sea. *Bull. Jap. Fish. Res. Edu. Agen*. 49, 27-34.

Yoshida, T., Ohama, N., Nakajima, J., Kidokoro, S., Mizoi, J., Nakashima, K., Maruyama, K., Kim, J. M., Seki, M., Todaka, D., Osakabe, Y., Sakuma, Y., Schöffl, F., Shinozaki, K., Yamaguchi-Shinozaki, K. 2011. *Arabidopsis* HsfA1 transcription factors function as the main positive regulators in heat

shock-responsive gene expression. *Mol. Genet. Genom*. 286, 321-332.

Yoshida, T., Sakuma, Y., Todaka, D., Maruyama, K., Qin, F., Mizoi, J., Kidokoro, S., Fujita, Y., Shinozaki, K., Yamaguchi-Shinozaki, K. 2008. Functional analysis of an *Arabidopsis* heat-shock transcription factor HsfA3 in the transcriptional cascade downstream of the DREB2A stress-regulatory system. *Biochem. Biophys. Res. Commun.* 368, 515-21.

Yu, X., Mo, Z., Tang, X. 2021. Genome-wide analysis of *HSP70* gene superfamily in *Pyropia yezoensis* (Bangiales, Rhodophyta): identification, characterization and expression profiles in response to dehydration stress. *BMC Plant Biol*. 21, 435.

Zhou, X., Wang, P., Yan, B., Li, X., Yi, L. 2011. Characterization and expression patterns of two 70-kDa heat shock protein genes in the intertidal red alga *Porphyra yezoensis*. *Bot. Mar.* 54, 447-455.

Zoong, L. Z., Sah, S., Persaud, L., Li, J., Gao, W., Raja Reddy, K., Narayanan, S. 2021. Alterations in the leaf lipidome of *Brassica carinata* under high-temperature stress. *BMC Plant Biol.* 21, 404.

Figure legends

Figure 1. Triphasic life cycle in *Neopyropia yezoensis* containing three different generations: gametophyte, sporophyte and conchosporophyte. Scale bars: gametophyte, 0.5 cm; sporophyte and conchosporophyte, 50 μm; conchospore and its germinating organisms, 15 μm.

Figure 2. HTR2 homologs are conserved in the Bangiales. DDBJ/EMBL/GenBank accession numbers of homologs are indicated after species names. HTR2 homologs from *Neopyropia yezoensis* are highlighted and boxed. The bootstrap values with 1000 replicates are indicated at the nodes of the tree. Bar, 0.1 substitutions per site.

Figure 3. Conservation of the Bangiales cysteine-rich (BCR) motif in HTR2 homologs from *Neopyropia yezoensis*, *Neopyropia seriata*, and *Porphyra umbilicalis*. Cysteine residues and amino acids conserved in all 11 proteins are highlighted in black and darkblue (with white characters), respectively. Yellow backgrounds indicate amino acids conserved in 7 to 10 proteins. The position of the BCR motif is indicated by a red bar. The amino acid position numbers are indicated on the right.

Figure 4. Cycle threshold (Ct) values and gene expression stability values M of candidate reference genes in three life cycle generations of *Neopyropia yezoensis*. (A) Ct values of candidate reference genes. Boxes show the median (center lines), Q1 (lower outline), Q3 (upper outline), and 1.5 times the interquartile range above Q3 and below Q1 (whiskers). Data were derived from 3 replicates of 27 culture samples. (B) M was calculated by stepwise exclusion of the least stable gene in three generations using geNorm. In each plot, the least stable gene is on the left and the most stable gene is on the right. Data were derived from 3 replicates of 22 culture samples for each generation. G, gametophyte; S, sporophyte; CS, conchosporophyte.

Figure 5. Temperature-dependent expression patterns of *NyMBF1* in *Neopyropia yezoensis* gametophytes. Relative mRNA levels at 5, 15, and 25ºC were normalized using *GAPDH*, *EF1α*, or *eIF4A* as the reference gene. There was a statistically significant interaction between the effects of time and temperature on relative mRNA level as defined by *Tukey's* test ($p < 0.05$) in two-way ANOVA. Significant differences in expression level among the three life cycle generations from triplicate independent replicates are shown in Table 4.

Figure 6. Temperature-dependent expression patterns of *NyMBF1* in *Neopyropia*

yezoensis sporophytes. Relative mRNA levels at 5, 15, and 25ºC were normalized using *GAPDH*, *EF1α*, or *eIF4A* as the reference gene. There was a statistically significant interaction between the effects of time and temperature on relative mRNA level as defined by *Tukey's* test ($p < 0.05$) in two-way ANOVA. Significant differences in expression level among the three life cycle generations from triplicate independent replicates are shown in Table 4.

Figure 7. Temperature-dependent expression patterns of *NyMBF1* in *Neopyropia yezoensis* conchosporophytes. Relative mRNA levels at 5, 15, and 25ºC were normalized using *GAPDH*, *EF1α*, or *eIF4A* as the reference gene. There was a statistically significant interaction between the effects of time and temperature on relative mRNA level as defined by *Tukey's* test ($p < 0.05$) in two-way ANOVA. Significant differences in expression level among the three life cycle generations from triplicate independent replicates are shown in Table 4.

Figure 8. Temperature-dependent expression patterns of *NyHTR2* and *NyHTR2L* with temporal comparisons over three life cycle generations of *Neopyropia yezoensis*. The relative mRNA levels were normalized using *eIF4A* as the reference gene. In the box plots, values on the Y axis represent the fold change of relative quantification of each gene. There was a statistically significant interaction

between the effects of time and temperature on relative mRNA level as defined by *Tukey's* test ($p < 0.05$) in two-way ANOVA. Significant differences in expression level among the three life cycle generations from triplicate independent replicates are shown in Table 5. G, gametophyte; S, sporophyte; CS, conchosporophyte.

Figure 9. Temperature-dependent expression patterns of *NyHSP70-1* and *NyHSP70-2* with temporal comparisons in three life cycle generations of *Neopyropia yezoensis*. Relative mRNA levels were normalized using *eIF4A* as the reference gene. There was a statistically significant interaction between the effects of time and temperature on relative mRNA level as defined by *Tukey's* test ($p < 0.05$) in two-way ANOVA. Significant differences in expression level among the three life cycle generations from triplicate independent replicates are shown in Table 6. G, gametophyte; S, sporophyte; CS, conchosporophyte.

Figure 10. Effect of dark treatment on the second expression peak of *NyHTR2* and *NyHTR2L* in three life cycle generations of *Neopyropia yezoensis* at 25°C. Gene expression in the light and the dark, at 8 and 12 h after heat stress exposure, was compared. Relative mRNA levels were normalized using *eIF4A* as the reference gene. In the box plots, values on the Y axis represent the fold change of relative quantification of each gene. Different letters denote significant differences in

expression level among the three life cycle generations from triplicate independent replicates as defined by *Tukey's* test ($p < 0.05$) in one-way ANOVA. L, light; D, dark; G, gametophyte; S, sporophyte; CS, conchosporophyte.

Figure 11. Effect of dark treatment on the second expression peak of *NyMBF1*, *NyHSP70-1*, and *NyHSP70-2* in three life cycle generations of *Neopyropia yezoensis* at 25°C. Gene expression in the light and dark, at 8 and 12 h after heat stress exposure, were compared. Relative mRNA levels were normalized using *eIF4A* as the reference gene. In the box plots, values on the Y axis represent the fold change of relative quantification of each gene. Different letters denote significant differences in expression level among the three life cycle generations from triplicate independent replicates as defined by *Tukey's* test ($p < 0.05$) in one-way ANOVA. L, light; D, dark; G, gametophyte; S, sporophyte; CS, conchosporophyte.

Figure 12. Effects of changes in membrane physical state on *NyHTR2* and *NyHTR2L* expression in three life cycle generations of *Neopyropia yezoensis*. The algae were treated with 2.5 mM BA and 4% DMSO at 15 ºC for 5, 15, and 30 min, and the expression of *NyHSP70-1* and *NyHSP70-2* was compared with their expression at 25ºC. Relative mRNA levels were normalized using *eIF4A* as the

reference gene. In the box plots, values on the Y axis represent the fold change of relative quantification of each gene. There was a statistically significant interaction between the effects of time and BA or DMSO treatment on relative mRNA level (except effects of changes in membrane physical state on *NyHTR2L* expression in CS) as defined by *Tukey's* test ($p < 0.05$) in two-way ANOVA. Different letters represent significant differences. G, gametophyte; S, sporophyte; CS, conchosporophyte.

Figure 13. Effects of changes in membrane physical state on *NyMBF1*, *NyHSP70-1*, and *NyHSP70-2* expression in three life cycle generations of *Neopyropia yezoensis*. The algae were treated with 2.5 mM BA and 4% DMSO at 15ºC for 5, 15, and 30 min, and the expression of *NyHSP70-1* and *NyHSP70-2* was compared with their expression at 25ºC. Relative mRNA levels were normalized using *eIF4A* as the reference gene. In thebox plots, values on the Y axis represent the fold change of relative quantification of each gene. There was a statistically significant interaction between the effects of time and BA or DMSO treatment on relative mRNA level as defined by *Tukey's* test ($p < 0.05$) in two-way ANOVA. Different letters represent significant differences. G, gametophyte; S, sporophyte; CS, conchosporophyte.

Figure 14. Induction of *NyHSP70-1* by exposure to 0ºC in three life cycle generations of *Neopyropia yezoensis*. Generations were incubated at 0℃ for 15, 30, 60, and 120 min, and expression of *NyHTR2*, *NyHTR2L*, *NyMBF1*, *NyHSP70-1*, and *NyHSP70-2* was examined. Relative mRNA levels were normalized using *eIF4A* as the reference gene. In the box plots, values on the Y axis represent the fold change of relative quantification of each gene. There was a statistically significant interaction between the effects of time and genes on relative mRNA level as defined by *Tukey's* test ($p < 0.05$) in two-way ANOVA. Different letters represent significant differences. G, gametophyte; S, sporophyte; CS, conchosporophyte.

Figure 15. Involvement of membrane fluidization in dark-induced gene expression in three life cycle generations of *Neopyropia yezoensis*. The algae were treated with 2.5 mM BA, and expression of *NyHTR2*, *NyHTR2L*, *NyMBF1*, *NyHSP70-1*, and *NyHSP70-2* was examined at 8 and 12 h after heat stress (25ºC) exposure under continual light. Relative mRNA levels were normalized using *eIF4A* as the reference gene. In the box plots, values on the Y axis represent the fold change of relative quantification of each gene. There was a statistically significant interaction between the effects of time and genes on relative mRNA level as defined by *Tukey's* test ($p < 0.05$) in two-way ANOVA. Different letters represent significant

differences. G, gametophyte; S, sporophyte; CS, conchosporophyte.

Figure 16. Reduction of the dark-induced second expression peak by membrane rigidification in three life cycle generations of *Neopyropia yezoensis*. The algae were treated with 4% DMSO, and expression of *NyHTR2*, *NyHTR2L*, *NyMBF1*, *NyHSP70-1*,and *NyHSP70-2* was examined 8 and 12 h after heat stress exposure (25℃) in the dark. Relative mRNA levels were normalized using *eIF4A* as the reference gene. In the box plots, values on the Y axis represent the fold change of relative quantification of each gene. There was a statistically significant interaction between the effects of time and genes on relative mRNA level as defined by *Tukey's* test ($p < 0.05$) in two-way ANOVA. Different letters represent significant differences. G, gametophyte; S, sporophyte; CS, conchosporophyte.

Table 1. Sequences of primers for candidates of reference genes used for qRT-PCR

Gene	Primer sequence (5' to 3')	Amplicon length (bp)	Efficiency (%)	Correlation coefficient (R^2)
GAPDH	CCAACAAGTGGGAGTAAGCG	104	99.1	0.9970
	GGACAGAACCGAACAGCGTA			
EF1α	TTTTGGTGGCACTGCTGAT	141	98.0	0.9975
	TACACGCACAAGTTGGGGA			
eIF4A	GCTTTCTGTCTGGACGAGG	181	101.0	0.9992
	TCTTCACAAGGATGCGGAT			

Table 2. Expression stability analysis of four reference genes by NormFinder in three life cycle generations of *Neopyropia yezoensis*

Gametophyte			Sporophyte			Conchosporophyte		
Rank	**Gene**	**Stability value**	**Rank**	**Gene**	**Stability value**	**Rank**	**Gene**	**Stability value**
1	*eIF4A*	0.137	1	*eIF4A*	0.278	1	*eIF4A*	0.134
2	*EF1α*	0.208	2	*GAPDH*	0.348	2	*GAPDH*	0.300
3	*GAPDH*	0.544	3	*EF1α*	0.403	3	*EF1α*	0.326

Table 3. Sequences of primers for heat stress-inducible genes used for qRT-PCR

Primer name	Primer sequence (5' to 3')	Annealing temperature (°C)	Product size (bp)
Q-NyMBF1-F	TCGAGCTTGGAGAGATTGGT	58	114
Q-NyMBF1-R	GAAGAAGGCGGATGTCTCTG		
Q-NyHTR2-F	CACACCTACGCGTGCTACTT	59	134
Q-NyHTR2-R	CACTTGTCGCACTTGCACTT		
Q-NyHTR2L-F	CATACCTACCCGTGCTGGTT	60	134
Q-NyHTR2L-R	CACACGTCACACTTGCACTG		
Q-NyHSP70-1-F	GGTTCGCACCCCAACATCAC	59	112
Q-NyHSP70-1-R	TCACAGCCACAACCTCTCACC		
Q-NyHSP70-2-F	CATTGGTGACTCAGCGAAGA	59	143
Q-NyHSP70-2-R	CCTTCTGCACCACCTTGAAT		

Table 4. Temperature-dependent gene expression profiles of *NyMBF1* in three life cycle generations of *Neopyropia yezoensis* normalized using reference genes

Generation	Reference gene	Temperature	Duration (h)							
			0	**0.5**	**1**	**2**	**4**	**6**	**8**	**12**
G	***GAPDH***	5ºC	1 ± 0^{a}	1.32 ± 0.07^{a}	1.85 ± 0.09^{a}	2.09 ± 0.04^{a}	1.49 ± 0.04^{a}	3.71 ± 0.13^{a}	6.3 ± 0.97^{ab}	20.2 ± 2.55^{c}
		15ºC	1 ± 0^{a}	0.76 ± 0.08^{a}	1.11 ± 0.13^{a}	1.71 ± 0.16^{a}	10.92 ± 1.37^{b}	24.75 ± 1.75^{cd}	136.98 ± 2.85^{f}	21.38 ± 1.88^{cd}
		25ºC	1 ± 0^{a}	1.11 ± 0.12^{a}	2.56 ± 0.1^{a}	4.87 ± 0.11^{ab}	26.35 ± 2.06^{d}	41.86 ± 3.01^{e}	143.54 ± 6.27^{g}	20.05 ± 2.07^{c}
	EF1α	5ºC	1 ± 0^{a}	2.75 ± 0.08^{g}	3.95 ± 0.18^{j}	2.33 ± 0.17^{ef}	1.28 ± 0.22^{ab}	2.03 ± 0.19^{cde}	1.18 ± 0.17^{a}	1.12 ± 0.13^{a}
		15ºC	1 ± 0^{a}	1.32 ± 0.09^{ab}	2.26 ± 0.17^{def}	1.67 ± 0.2^{bc}	1.65 ± 0.2^{bc}	1.77 ± 0.19^{c}	1.87 ± 0.18^{cd}	1.06 ± 0.16^{a}
		25ºC	1 ± 0^{a}	1.74 ± 0.15^{c}	2.5 ± 0.14^{fg}	3.54 ± 0.12^{ij}	6.27 ± 0.22^{l}	3.22 ± 0.23^{i}	4.7 ± 0.41^{k}	1.07 ± 0.06^{a}
	eIF4A	5ºC	1 ± 0^{a}	1.9 ± 0.59^{a}	1.57 ± 0.12^{ab}	1.64 ± 0.12^{ab}	1.85 ± 0.18^{ab}	1.4 ± 0.25^{a}	1.65 ± 0.26^{a}	3.44 ± 0.1^{ab}
		15ºC	1 ± 0^{a}	2.2 ± 0.18^{ab}	1.92 ± 0.14^{b}	2.89 ± 0.15^{ab}	3.15 ± 0.1^{ab}	3.2 ± 0.15^{ab}	3.71 ± 0.27^{ab}	3.26 ± 0.22^{ab}
		25ºC	1 ± 0^{a}	2.61 ± 0.37^{ab}	6.15 ± 0.14^{bc}	43.27 ± 3.58^{f}	19.07 ± 1.6^{e}	10.94 ± 1.7^{d}	55.72 ± 5.15^{g}	10.4 ± 1^{cd}
S	***GAPDH***	5ºC	1 ± 0^{a}	1.05 ± 0.27^{a}	1.07 ± 0.15^{a}	1.15 ± 0.13^{a}	1.51 ± 0.16^{a}	2.55 ± 0.25^{ab}	5.23 ± 0.79^{cd}	9.44 ± 1.18^{ef}
		15ºC	1 ± 0^{a}	0.97 ± 0.09^{a}	1.23 ± 0.15^{a}	1.47 ± 0.23^{ab}	3.25 ± 0.34^{abc}	7.57 ± 0.34^{de}	7.18 ± 0.86^{de}	2.43 ± 0.15^{ab}
		25ºC	1 ± 0^{a}	2.15 ± 0.2^{ab}	4.48 ± 0.42^{bc}	8.03 ± 0.31^{e}	10.88 ± 0.66^{f}	18.68 ± 2.05^{g}	17.74 ± 1.84^{g}	7.71 ± 1.09^{e}
	EF1α	5ºC	1 ± 0^{a}	1.54 ± 0.22^{a}	2.99 ± 0.28^{ab}	3.31 ± 0.27^{ab}	3.12 ± 0.23^{ab}	1.34 ± 0.2^{a}	1.41 ± 0.15^{a}	1.05 ± 0.18^{a}
		15ºC	1 ± 0^{a}	1.01 ± 0.23^{a}	7.48 ± 0.51^{de}	5.66 ± 0.49^{bcd}	3.59 ± 0.49^{abc}	2.39 ± 0.22^{a}	1.32 ± 0.07^{a}	1.15 ± 0.17^{a}
		25ºC	1 ± 0^{a}	2.89 ± 0.36^{ab}	32.13 ± 4.36^{g}	12.52 ± 0.47^{f}	10.19 ± 1.09^{ef}	6.6 ± 0.43^{cd}	2.45 ± 0.37^{ab}	1.43 ± 0.22^{a}
	eIF4A	5ºC	1 ± 0^{a}	0.84 ± 0.08^{a}	0.96 ± 0.08^{a}	0.93 ± 0.09^{a}	1 ± 0.04^{a}	0.8 ± 0.15^{a}	0.98 ± 0.24^{a}	2.41 ± 0.2^{a}
		15ºC	1 ± 0^{a}	1.08 ± 0.03^{a}	1.61 ± 0.37^{a}	1.92 ± 0.32^{a}	2.15 ± 0.2^{a}	2.62 ± 0.15^{a}	2.23 ± 0.18^{a}	2.34 ± 0.17^{a}
		25ºC	1 ± 0^{a}	3.24 ± 0.35^{a}	10.28 ± 1.21^{bc}	33.57 ± 2.84^{e}	13.28 ± 1.99^{cd}	13.86 ± 1.51^{d}	32.86 ± 2.29^{e}	8.21 ± 0.26^{b}
CS	***GAPDH***	5ºC	1 ± 0^{ab}	0.86 ± 0.07^{a}	1.76 ± 0.2^{ab}	1.74 ± 0.07^{ab}	3.54 ± 0.11^{abc}	3.52 ± 0.45^{abc}	11.61 ± 0.58^{d}	4.93 ± 0.32^{bc}
		15ºC	1 ± 0^{ab}	1.52 ± 0.15^{ab}	1.38 ± 0.28^{ab}	1.79 ± 0.1^{ab}	2.79 ± 0.16^{abc}	3.03 ± 0.08^{abc}	6.48 ± 0.13^{c}	4.13 ± 0.12^{abc}
		25ºC	1 ± 0^{ab}	1.85 ± 0.15^{ab}	2.4 ± 0.27^{ab}	3.14 ± 0.16^{abc}	6.61 ± 0.65^{c}	12.51 ± 2.23^{d}	41.25 ± 2.69^{e}	69.79 ± 4.62^{f}
	EF1α	5ºC	1 ± 0^{a}	4.69 ± 0.3^{ef}	7.71 ± 0.77^{g}	2.36 ± 0.31^{bcd}	10.47 ± 1.53^{h}	5.07 ± 0.47^{f}	3.25 ± 0.23^{cdef}	1.16 ± 0.14^{ab}
		15ºC	1 ± 0^{a}	1.53 ± 0.18^{ab}	1.67 ± 0.15^{abc}	3.7 ± 0.41^{def}	4.18 ± 0.44^{def}	3.97 ± 0.26^{def}	4.24 ± 0.73^{def}	1.79 ± 0.3^{abc}
		25ºC	1 ± 0^{a}	2.45 ± 0.5^{abcd}	13.21 ± 1.84^{i}	9.54 ± 0.87^{gh}	7.77 ± 0.73^{g}	4.62 ± 0.46^{ef}	3.77 ± 0.17^{def}	2.8 ± 0.19^{bcde}
	eIF4A	5ºC	1 ± 0^{a}	1.06 ± 0.18^{a}	1.69 ± 0.15^{ab}	0.73 ± 0.03^{a}	0.84 ± 0.11^{a}	1.21 ± 0.19^{a}	1.48 ± 0.16^{ab}	1.22 ± 0.11^{a}
		15ºC	1 ± 0^{a}	0.86 ± 0.13^{a}	0.77 ± 0.09^{a}	0.87 ± 0.11^{a}	1.18 ± 0.13^{a}	1.34 ± 0.13^{a}	1.34 ± 0.11^{a}	1.48 ± 0.03^{ab}
		25ºC	1 ± 0^{a}	1.27 ± 0.05^{a}	2.55 ± 0.09^{bc}	7.63 ± 1.12^{f}	4.06 ± 0.29^{de}	4.2 ± 0.34^{e}	10.99 ± 0.85^{g}	3 ± 0.75^{cd}

Mean values ± SD were calculated from triplicate experiments, and there was a statistically significant interaction between the effects of time and temperature on relative mRNA level as defined by *Tukey's* test ($p < 0.05$) in two-way ANOVA. Different letters represent significant differences. G, gametophyte; S, sporophyte; CS, conchosporophyte.

Table 5. Gene expression profiles of *NyHTR2* and *NyHTR2L* in three generations of *Neopyropia yezoensis* under heat stress normalized using *eIF4A* as the reference gene

Gene	Generation	Temperature	Duration (h)							
			0	**0.5**	**1**	**2**	**4**	**6**	**8**	**12**
NyHTR2	G	5ºC	1 ± 0^{b}	0.03 ± 0.01^{a}	0.07 ± 0.02^{a}	0.28 ± 0.05^{a}	0.6 ± 0.2^{ab}	0.67 ± 0.06^{ab}	0.86 ± 0.09^{ab}	2.67 ± 0.45^{d}
		15ºC	1 ± 0^{b}	1.47 ± 0.21^{bc}	0.94 ± 0.25^{b}	0.81 ± 0.28^{b}	1.21 ± 0.16^{bc}	1.06 ± 0.38^{bc}	1.3 ± 0.28^{bc}	1.43 ± 0.3^{c}
		25ºC	1 ± 0^{b}	2.27 ± 0.62^{d}	3.63 ± 0.94^{de}	12.46 ± 1.97^{g}	3.71 ± 1.19^{de}	4.24 ± 1.02^{e}	12.19 ± 2.55^{g}	6.96 ± 1.44^{f}
NyHTR2L	G	5ºC	1 ± 0^{ab}	0.07 ± 0.02^{a}	0.51 ± 0.04^{a}	2.99 ± 0.15^{ab}	2.77 ± 0.43^{ab}	0.9 ± 0.17^{ab}	0.01 ± 0^{a}	5.11 ± 0.49^{b}
		15ºC	1 ± 0^{ab}	2.33 ± 0.95^{ab}	2.35 ± 1^{ab}	4.93 ± 0.35^{b}	5.43 ± 0.4^{b}	3.22 ± 0.84^{b}	1.48 ± 0.08^{ab}	4.14 ± 0.94^{b}
		25ºC	1 ± 0^{ab}	8.05 ± 1.21^{c}	35.21 ± 1.52^{e}	64.43 ± 4.05^{fg}	16.87 ± 1.29^{d}	27.82 ± 5.89^{e}	73.19 ± 6.37^{g}	54.74 ± 4.37^{f}
	S	5ºC	1 ± 0^{b}	1 ± 0.1^{b}	0.97 ± 0.1^{b}	0.88 ± 0.08^{b}	1.37 ± 0.02^{b}	0.51 ± 0.09^{a}	0.42 ± 0.11^{a}	0.98 ± 0.05^{b}
		15ºC	1 ± 0^{b}	1.43 ± 0.08^{bc}	1.36 ± 0.32^{bc}	1.59 ± 0.44^{bc}	1.42 ± 0.15^{bc}	1.75 ± 0.11^{bc}	$1.92 \pm 0.2b^{c}$	2.05 ± 0.3^{c}
		25ºC	1 ± 0^{b}	1.53 ± 0.16^{bc}	4.11 ± 0.57^{d}	7.04 ± 0.82^{e}	1.54 ± 0.28^{bc}	4.2 ± 0.53^{d}	11.54 ± 0.97^{f}	7.74 ± 0.23^{e}
	CS	5ºC	1 ± 0^{b}	0.73 ± 0.08^{ab}	1.29 ± 0.16^{bc}	0.5 ± 0.02^{ab}	0.35 ± 0.03^{a}	0.59 ± 0.06^{ab}	0.91 ± 0.1^{b}	0.93 ± 0.08^{b}
		15ºC	1 ± 0^{b}	0.48 ± 0.08^{a}	0.35 ± 0.04^{a}	0.48 ± 0.05^{a}	0.71 ± 0.01^{ab}	0.64 ± 0.06^{ab}	0.62 ± 0.02^{ab}	1.04 ± 0.03^{bc}
		25ºC	1 ± 0^{b}	0.64 ± 0.05^{ab}	1.41 ± 0.03^{c}	2.6 ± 0.46^{d}	1.66 ± 0.05^{cd}	1.29 ± 0.13^{bc}	4.93 ± 0.19^{e}	3.14 ± 0.24^{d}

Mean values ± SD were calculated from triplicate experiments, and there was a statistically significant interaction between the effects of time and temperature on relative mRNA level as defined by *Tukey's* test ($p < 0.05$) in two-way ANOVA. Different letters represent significant differences. G, gametophyte; S, sporophyte; CS, conchosporophyte.

Table 6. Gene expression profiles of *NyHSP70-1* and *NyHSP70-2* in three generations of *Neopyropia yezoensis* under heat stress normalized using *eIF4A* as the reference gene

Gene	Generation	Temperature	Duration (h)							
			0	**0.5**	**1**	**2**	**4**	**6**	**8**	**12**
NyHSP70-1	G	5ºC	1 ± 0^{a}	0.66 ± 0.08^{a}	0.59 ± 0.38^{a}	0.63 ± 0.44^{a}	0.72 ± 0.33^{a}	0.62 ± 0.19^{a}	0.75 ± 0.35^{a}	0.65 ± 0.52^{a}
		15ºC	1 ± 0^{a}	0.61 ± 0.2^{a}	0.95 ± 0.57^{a}	0.55 ± 0.15^{a}	0.61 ± 0.16^{a}	0.68 ± 0.25^{a}	0.93 ± 0.41^{a}	0.86 ± 0.57^{a}
		25ºC	1 ± 0^{a}	3.71 ± 1.55^{bc}	4.22 ± 0.79^{c}	13.45 ± 1.99^{e}	6.35 ± 0.93^{d}	2.89 ± 1.38^{b}	2.59 ± 0.52^{b}	2.73 ± 0.61^{b}
	S	5ºC	1 ± 0^{ab}	0.73 ± 0.11^{ab}	0.82 ± 0.2^{ab}	0.66 ± 0.29^{ab}	0.49 ± 0.17^{a}	0.6 ± 0.32^{ab}	0.34 ± 0.12^{a}	0.5 ± 0.25^{a}
		15ºC	1 ± 0^{ab}	0.69 ± 0.28^{ab}	0.64 ± 0.28^{ab}	0.73 ± 0.15^{ab}	0.7 ± 0.24^{ab}	0.64 ± 0.2^{ab}	0.65 ± 0.21^{ab}	1.06 ± 0.34^{ab}
		25ºC	1 ± 0^{ab}	2.08 ± 0.28^{bc}	4.71 ± 0.33^{d}	6.27 ± 1.26^{e}	2.39 ± 0.31^{c}	2.3 ± 0.31^{c}	1.52 ± 0.4^{b}	1.03 ± 0.34^{ab}
	CS	5ºC	1 ± 0^{b}	$0.85 \pm 0.12a^{b}$	1.12 ± 0.13^{b}	0.67 ± 0.11^{ab}	0.7 ± 0.35^{ab}	0.48 ± 0.18^{a}	0.55 ± 0.36^{ab}	0.35 ± 0.27^{a}
		15ºC	1 ± 0^{b}	1.07 ± 0.16^{b}	0.95 ± 0.11^{b}	1.14 ± 0.2^{b}	1.15 ± 0.1^{b}	1.16 ± 0.07^{b}	1.15 ± 0.15^{b}	1.12 ± 0.1^{b}
		25ºC	1 ± 0^{b}	3.67 ± 0.35^{d}	6.8 ± 0.56^{e}	3.62 ± 0.44^{d}	3.34 ± 0.2^{d}	3.29 ± 0.16^{d}	1.99 ± 0.08^{c}	1.79 ± 0.24^{bc}
NyHSP70-2	G	5ºC	1 ± 0^{a}	0.45 ± 0.08^{a}	0.44 ± 0.09^{a}	0.45 ± 0.23^{a}	0.16 ± 0.07^{a}	0.35 ± 0.44^{a}	0.4 ± 0.49^{a}	0.34 ± 0.24^{a}
		15ºC	1 ± 0^{a}	1.73 ± 1.36^{a}	1.36 ± 0.68^{a}	1.3 ± 0.91^{a}	1.37 ± 0.89^{a}	1.33 ± 0.87^{a}	1.34 ± 0.93^{a}	1 ± 0.34^{a}
		25ºC	1 ± 0^{a}	13.9 ± 1.85^{c}	50.2 ± 4.32^{ef}	126.33 ± 12.02^{g}	44.73 ± 4.05^{e}	21.79 ± 2.9^{d}	53.24 ± 4.7^{f}	5.52 ± 2.43^{b}
	S	5ºC	1 ± 0^{ab}	0.92 ± 0.14^{ab}	1.14 ± 0.24^{b}	0.82 ± 0.31^{ab}	0.7 ± 0.32^{a}	0.54 ± 0.38^{a}	0.59 ± 0.36^{a}	0.67 ± 0.35^{a}
		15ºC	1 ± 0^{ab}	1.23 ± 0.18^{b}	1.27 ± 0.19^{b}	1.16 ± 0.12^{b}	1.34 ± 0.32^{b}	1.28 ± 0.34^{b}	1.02 ± 0.06^{ab}	0.63 ± 0.25^{a}
		25ºC	1 ± 0^{ab}	7.27 ± 0.67^{c}	21.91 ± 1.67^{e}	28.51 ± 2.04^{f}	10.12 ± 0.79^{d}	11.52 ± 0.88^{d}	18.39 ± 1.83^{e}	1.88 ± 0.5^{b}
	CS	5ºC	1 ± 0^{b}	0.84 ± 0.12^{b}	0.6 ± 0.14^{ab}	0.51 ± 0.46^{ab}	0.14 ± 0.09^{a}	0.44 ± 0.38^{ab}	0.17 ± 0.08^{a}	0.32 ± 0.23^{a}
		15ºC	1 ± 0^{b}	0.36 ± 0.09^{a}	0.4 ± 0.16^{a}	0.27 ± 0.13^{a}	0.42 ± 0.18^{ab}	0.39 ± 0.15^{a}	0.34 ± 0.26^{a}	0.58 ± 0.16^{ab}
		25ºC	1 ± 0^{b}	3.96 ± 0.35^{c}	14.58 ± 1.15^{e}	7.66 ± 0.51^{d}	3.6 ± 0.41^{c}	1.8 ± 0.28^{b}	8.8 ± 0.74^{d}	1.49 ± 0.43^{b}

Mean values ± SD were calculated from triplicate experiments, and there was a statistically significant interaction between the effects of time and temperature on relative mRNA level as defined by *Tukey's* test ($p < 0.05$) in two-way ANOVA. Different letters represent significant differences. G, gametophyte; S, sporophyte; CS, conchosporophyte.

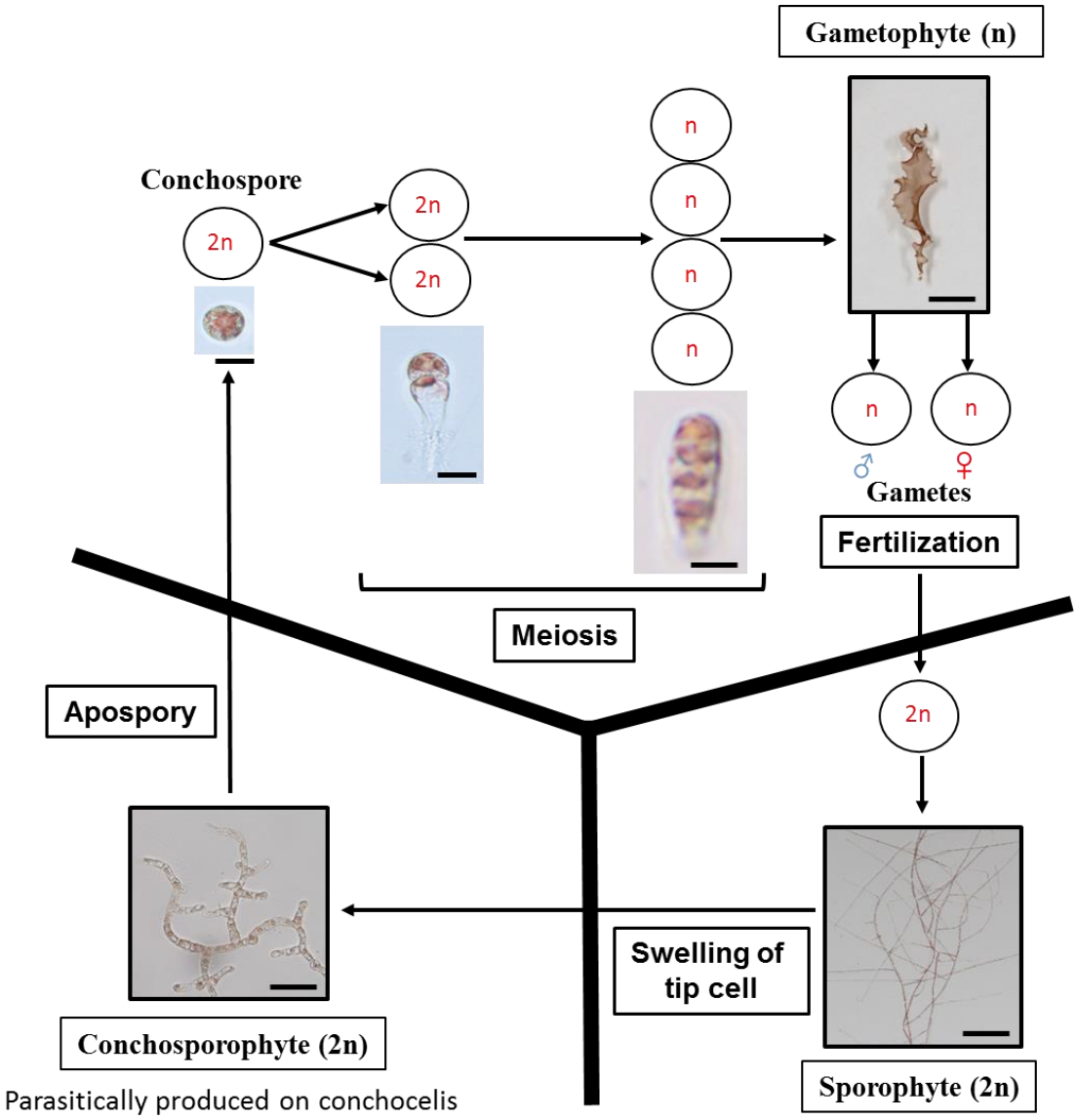
Gametophyte (n)
Conchospore
2n
2n
2n
n
n
n
n
n
n
♂
♀
Gametes
Fertilization
Meiosis
Apospory
2n
Swelling of tip cell
Conchosporophyte (2n)
Parasitically produced on conchocelis
Sporophyte (2n)

Figure 1

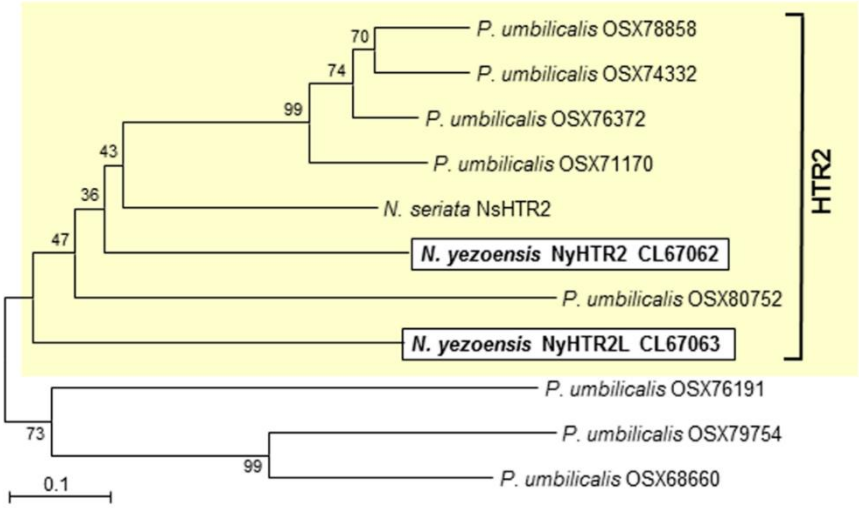
P. umbilicalis OSX78858
P. umbilicalis OSX74332
P. umbilicalis OSX76372
P. umbilicalis OSX71170
N. seriata NsHTR2
N. yezoensis NyHTR2 CL67062
P. umbilicalis OSX80752
N. yezoensis NyHTR2L CL67063
P. umbilicalis OSX76191
P. umbilicalis OSX79754
P. umbilicalis OSX68660
HTR2
70
74
99
43
36
47
73
99
0.1

Figure 2

```
NyHTR2    ------------------------------------------------------------
NyHTR2L   MPSGGRVAAAATRSPDQYKSSVTRPMVGGGECRPPTIPLRATSNQRRGNSPPFRDSPFPLS 61
NsHTR2    ------------------------------------------------------------
OSX76372  ------------------------------------------------------------
OSX78858  ------------------------------------------------------------
OSX74332  ------------------------------------------------------------
OSX71170  ------------------------------------------------------------
OSX80752  ------------------------------------------------------------
OSX79754  ------------------------------------------------------------
OSX68660  ------------------------------------------------------------
OSX76191  ------------------------------------------------------------

NyHTR2    ------------------MALSKTRFAALAVAVMTLLTAAAAPAADAAAAAA-------- 35
NyHTR2L   REHPPSPYPPRPPTSIVDMALSKLLMV---TALLAMLALPMASAA---------------- 103
NsHTR2    ------------------MAASKTLAAAFAVALLALLTLTAAAPAADTA--AA-------- 33
OSX76372  ------------------MAVPKSLFASLAVALLALLSVAAVSPTDAAV---A-------- 32
OSX78858  ------------------MAVPKSLFASLAVALLALLSVAAVSPADAAV---A-------- 32
OSX74332  ------------------MAVPKSLFASLAVALLALLSVAAVSPADAAV---A-------- 32
OSX71170  ------------------MVVSKSLFASLAVALLALLSVAAVSPADAAV---A-------- 32
OSX80752  ------------------MGAIKMLLVTAIVASLALLTVAASRPVAADDSADDMVDGAWPT 43
OSX79754  ------------------MAATKFLAL--LLTFVALLSVVAA-TD---------------- 24
OSX68660  ------------------MAATKALAL--LLTLVALVSLATA-TA---------------- 24
OSX76191  ------------------MAR-------FTLPLLVLLVAALV-PLVASAS----------- 24

NyHTR2    -DAATVEYESLRIEGLSDVADAPALTGLADRSPYGGGYGCRAYFKCQQKTEKVVAKHTYAC 95
NyHTR2L   ---LPV-----DREAVSAVADAPGLSAL--VR---ATEAC-SYFQCGSPTVEVVAKHTYPC 150
NsHTR2    -DAATAAYDALHVEGISGAAEAPALDGLTDRSG---YYRCRSYFVCGSKKVKVPVKHSHPC 90
OSX76372  -VQAASNPEALHIEGLSHADEEPALASLTGR-TR-YEGRCNSYFKCGTKSVTVVAKNSYLC 90
OSX78858  -VQAAPDPEALHIEGLSRADEEPALASLTVRS---PYGVCKGYFQCGTKSVTVEAKNTYLC 89
OSX74332  -VQAASDPEALHIEGLSRADEEPALASLTDRTVR-YGGICNRYFKCGTKSVTVVAKNSYLC 91
OSX71170  -VQAASDPEALHIEGLSRADEEPALASLTAHSYYGGHDTCNGYFKCGKKSVYVVAKASYLC 92
OSX80752  GADDDVPADVVVIGGHTPLNEAPGLADITARQQV-VAKKC-FYFKCNTKRVRRVVRQAWRC 102
OSX79754  ---VPPELEEEPVIGTSRVDAAPGLADITAVH----WGRCSSYFRCGRKLIFPKVKATYKC 78
OSX68660  ---VPAQ--GEDVFGSSTLIDAPGLSDIAAVR----ARKCSSYFPCGWRTATGQAKVSYKC 76
OSX76191  -----PA--SDVLSSVARTHGGPHDVSTVK------AGTCGGYVKCGKNTVKNTVKNSRYC 72
```

BCR motif

```
NyHTR2    YFKIASSAA--ARSAGGLCRPNPYGCV--AAKCGGWVKCKCDKCQTVSITYPVWCEQ     148
NyHTR2L   WFKVATGN---KGLAPDTCSPTPYDCVD-DATCKGWKQCKCDVCKTVKLTKKEYCKLPEE  206
NsHTR2    YYKEAPSIL-KSSRSSGLCRPDPYSCK--PATCIGWRKCTCDACKTVIFTHNIWCEK     144
OSX76372  YFKEAPSKA--SRSGSGRCNGLPYKCK--PAKCTGWRVCTCDQCKKVVFKVPIYCEK     143
OSX78858  YYKEAKSRS--T--RSSSCNTLPYNCK--PATCTGWRVCKCDQCKRVTFTFPIYCEQ     140
OSX74332  YYKEASYKI--GASGSGSCSSLPYNCK--RAKCTGWRVCTCNHCKRVTFTIPIYCEK     144
OSX71170  YFKEAESYR--GKAYSGECSSLPYNCK--PAKCPGWRKCTCDKCKKVLIKVPIYCEL     145
OSX80752  FFKVAFKITPKPKPTGSLCHPTPYACT--KSACGGWRRCLCDACKVVVFTYPVWCMKK    158
OSX79754  YFRTAASA--LPAKGPKRCGRFPYNCK--NAHCKGWKVCTCTKCFRARTRVPQWCEHP    132
OSX68660  YFKVAASLA-RPEAAKNGCAPHPYKCR--DAKCKGWKQCTCDKCFSAKTKVRVWCEHP    131
OSX76191  YFKLKTKPSPAKGDSKRNCKRAPYSCKRVASPCNGWYKCKCDECSTVKTEVDRWCLKK    130
```

Figure 3

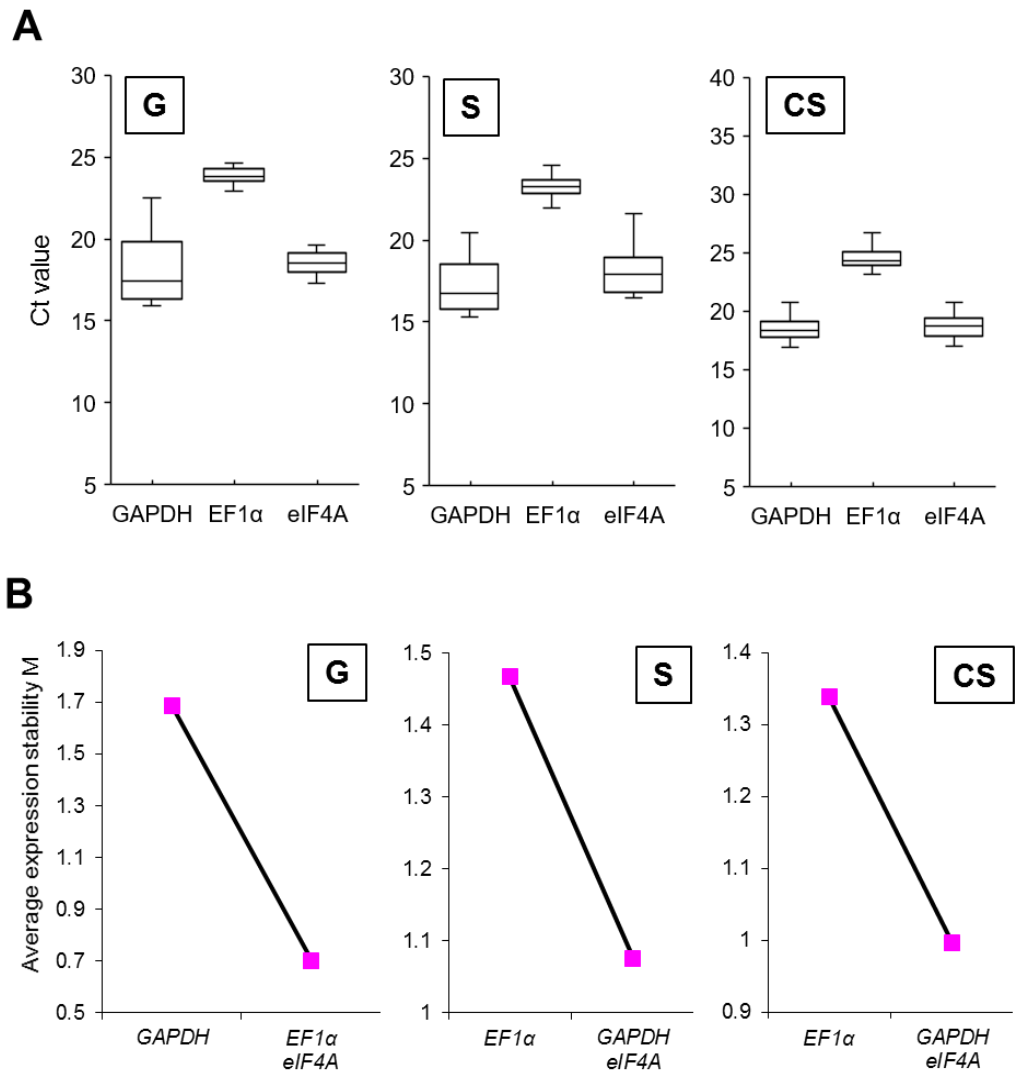
A
G
S
CS
Ct value
GAPDH
EF1α
eIF4A
B
Average expression stability M
GAPDH
EF1α
eIF4A

Figure 4

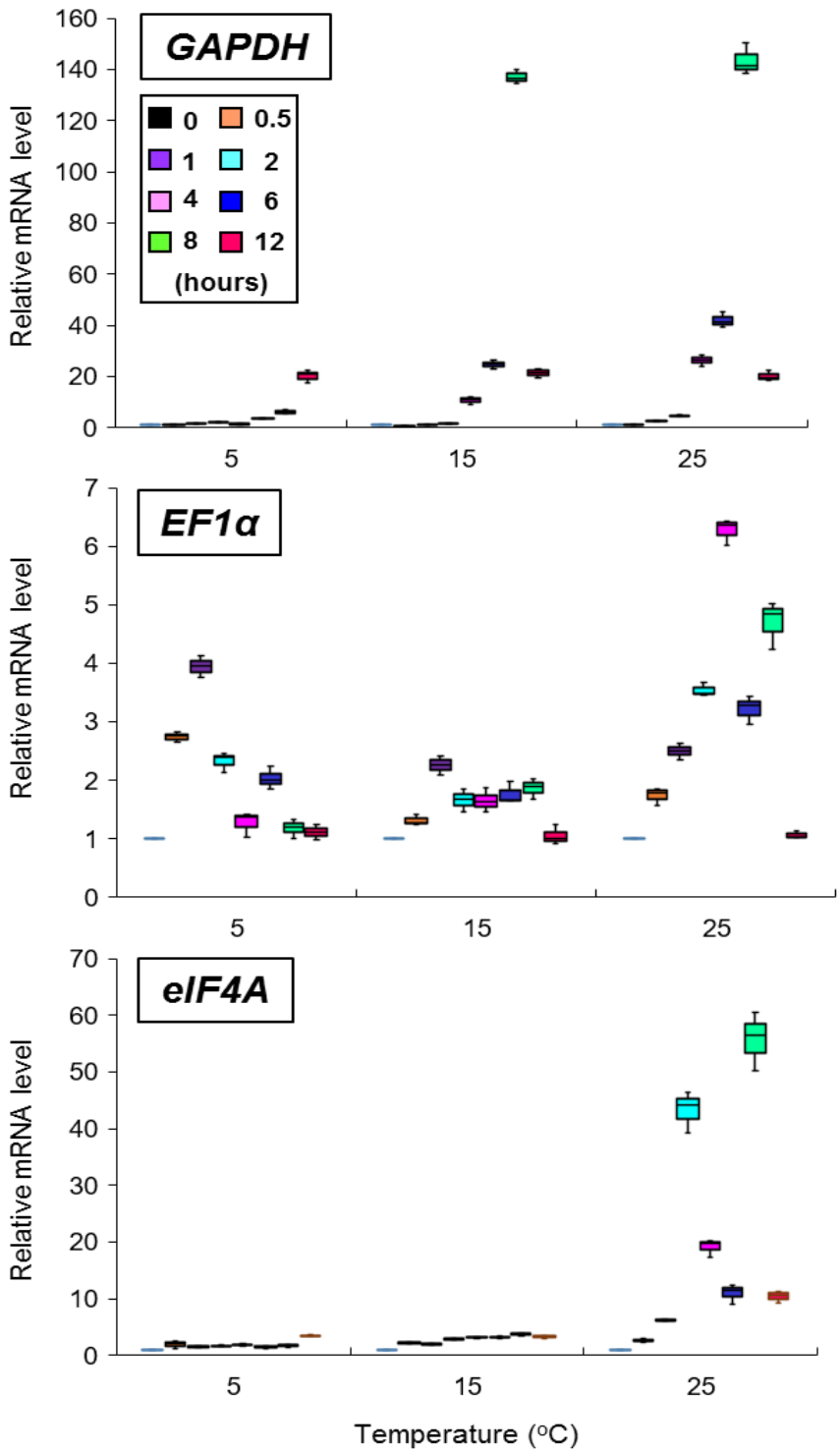
GAPDH
0
0.5
1
2
4
6
8
12
(hours)
Relative mRNA level
160
140
120
100
80
60
40
20
0
5
15
25
EF1α
Relative mRNA level
7
6
5
4
3
2
1
0
5
15
25
eIF4A
Relative mRNA level
70
60
50
40
30
20
10
0
5
15
25
Temperature (°C)

Figure 5

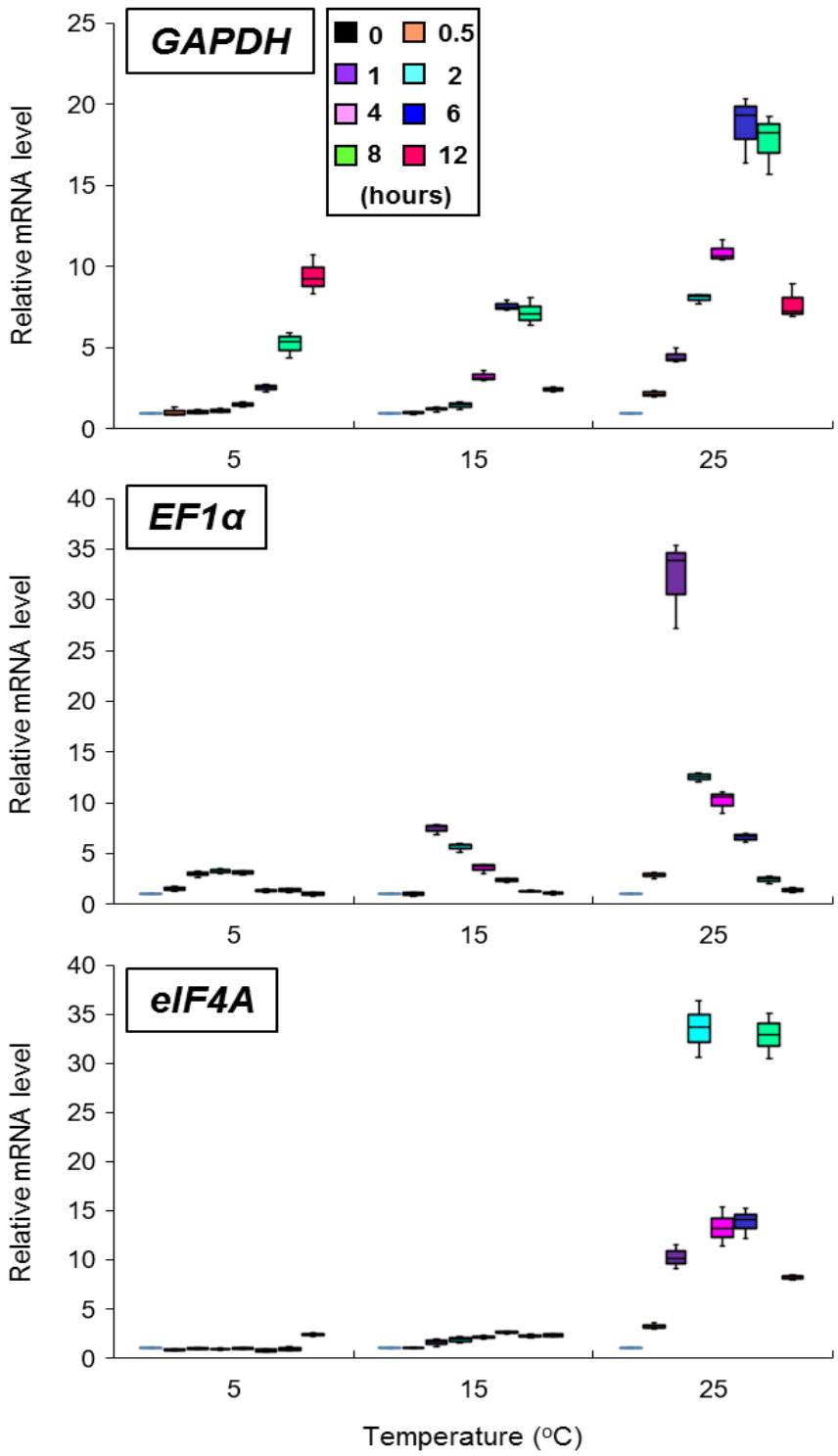
GAPDH
0
0.5
1
2
4
6
8
12
(hours)
Relative mRNA level
25
20
15
10
5
0
5
15
25
EF1α
40
35
30
25
20
15
10
5
0
eIF4A
Temperature (°C)

Figure 6

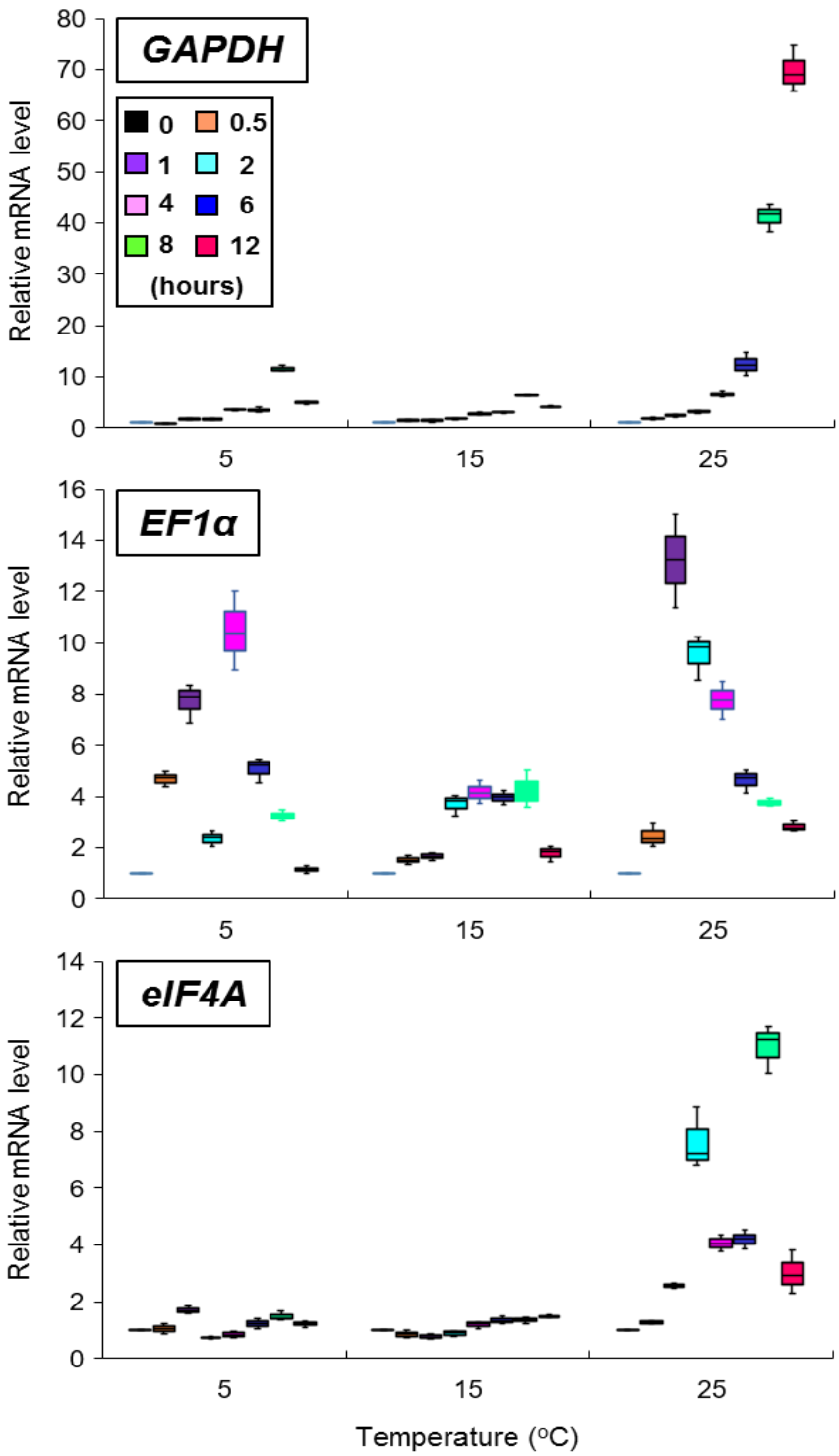
GAPDH
0
0.5
1
2
4
6
8
12
(hours)
Relative mRNA level
80
70
60
50
40
30
20
10
0
5
15
25
EF1α
16
14
12
10
8
6
4
2
0
elF4A
Temperature (°C)

Figure 7

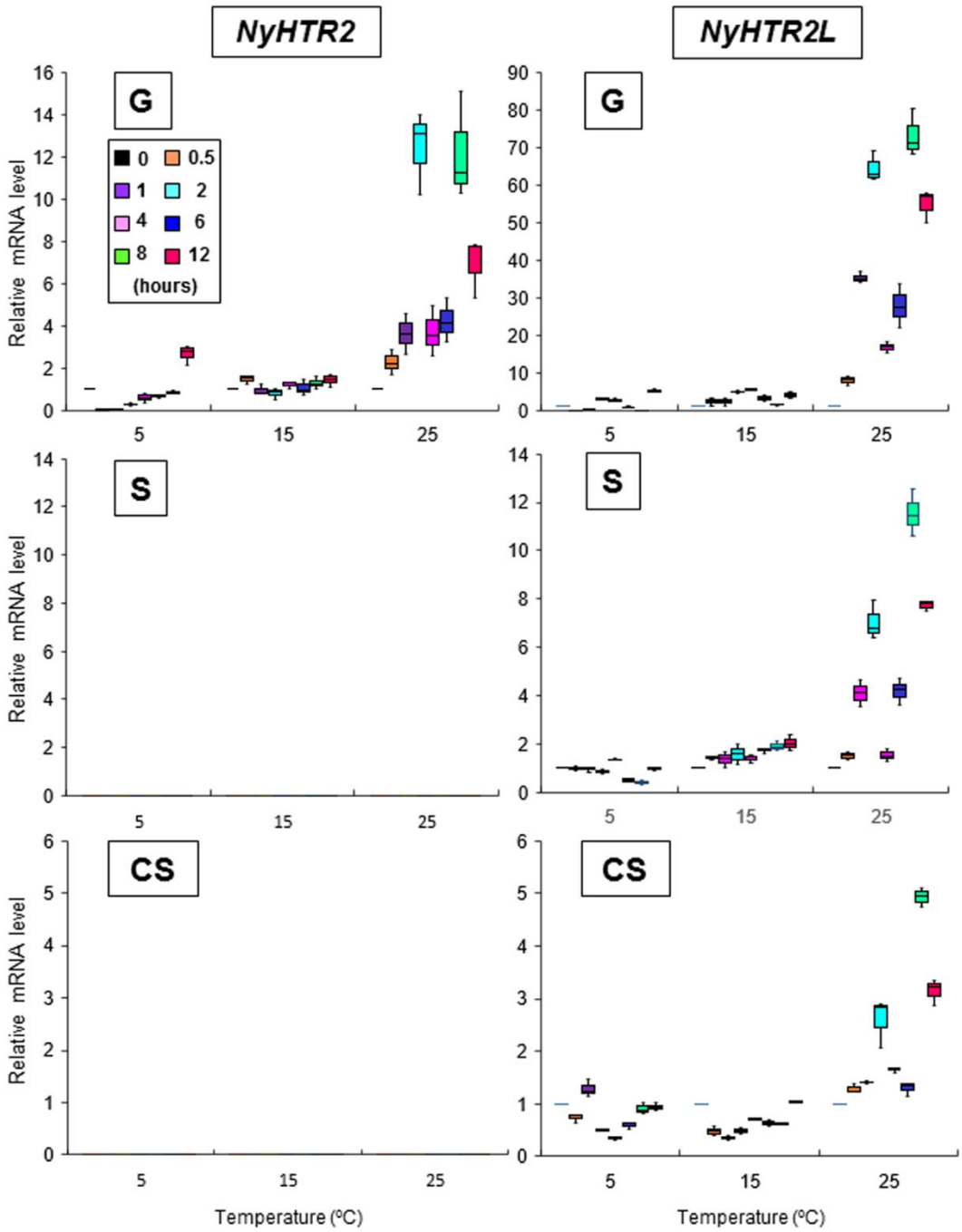
NyHTR2
NyHTR2L
G
S
CS
0
0.5
1
2
4
6
8
12
(hours)
Relative mRNA level
Temperature (ºC)
5
15
25

Figure 8

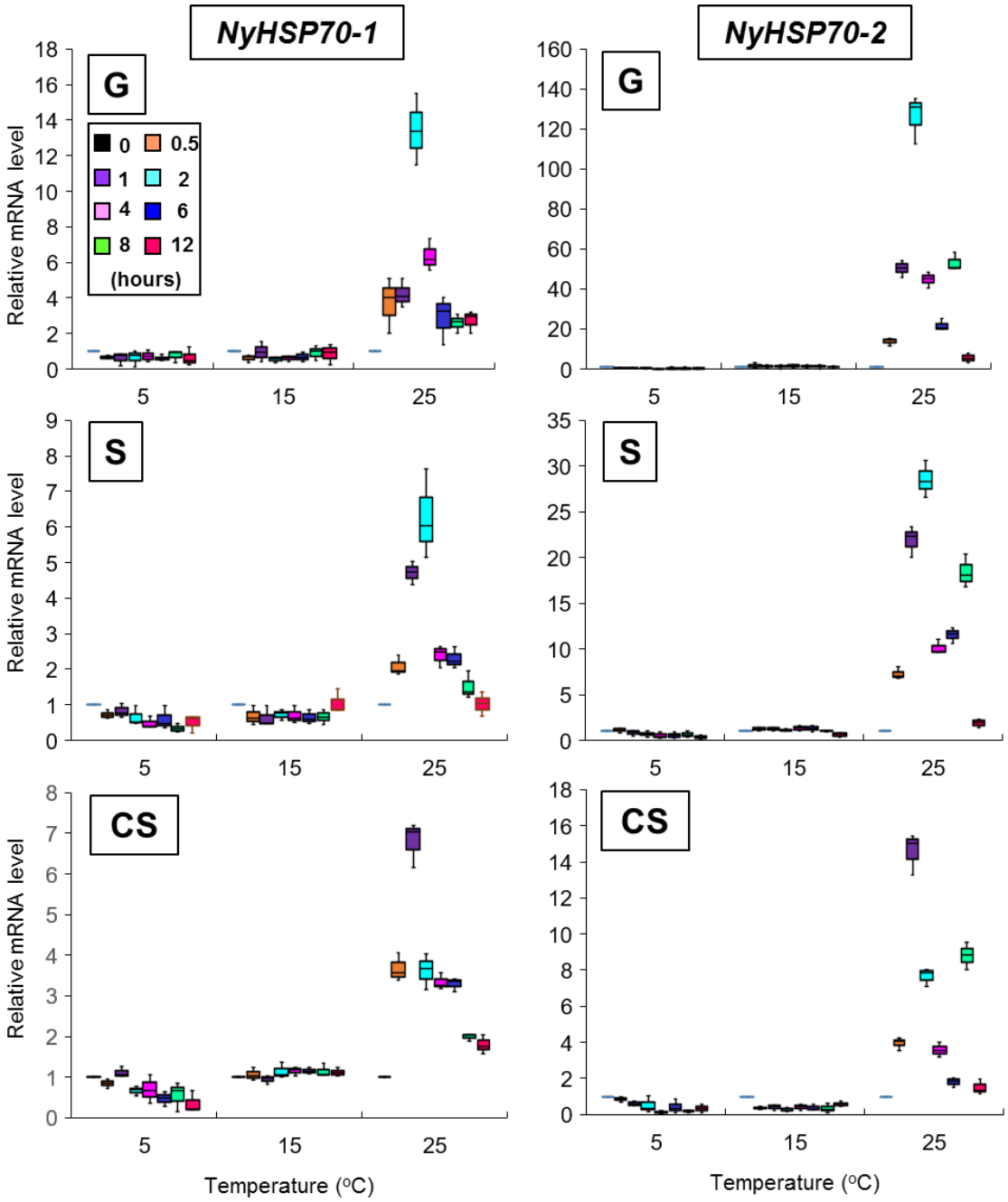
NyHSP70-1
NyHSP70-2
G
S
CS
0
0.5
1
2
4
6
8
12
(hours)
Relative mRNA level
Temperature (°C)
5
15
25

Figure 9

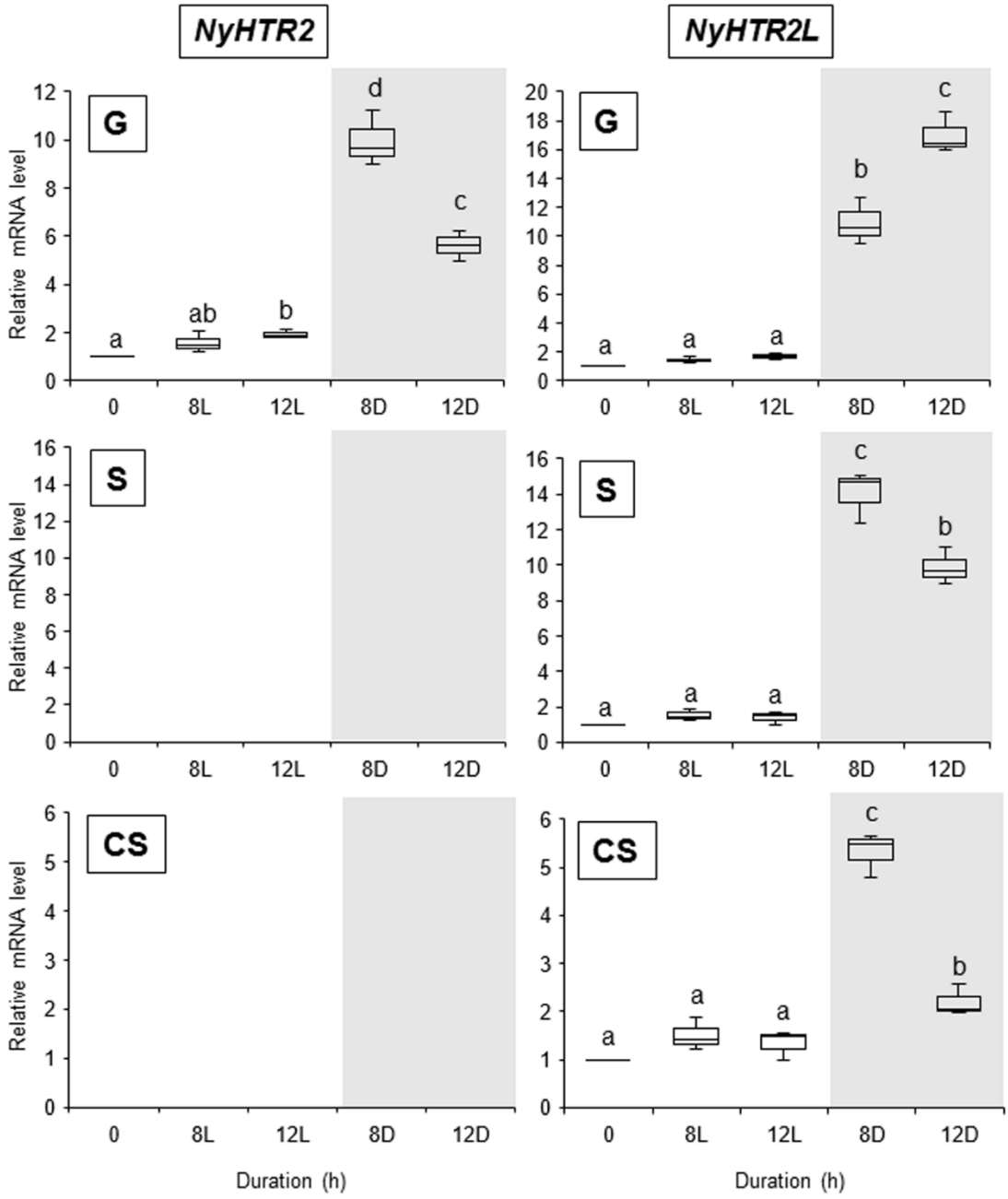
NyHTR2
NyHTR2L
G
S
CS
Relative mRNA level
Duration (h)
0
8L
12L
8D
12D
a
ab
b
c
d

Figure 10

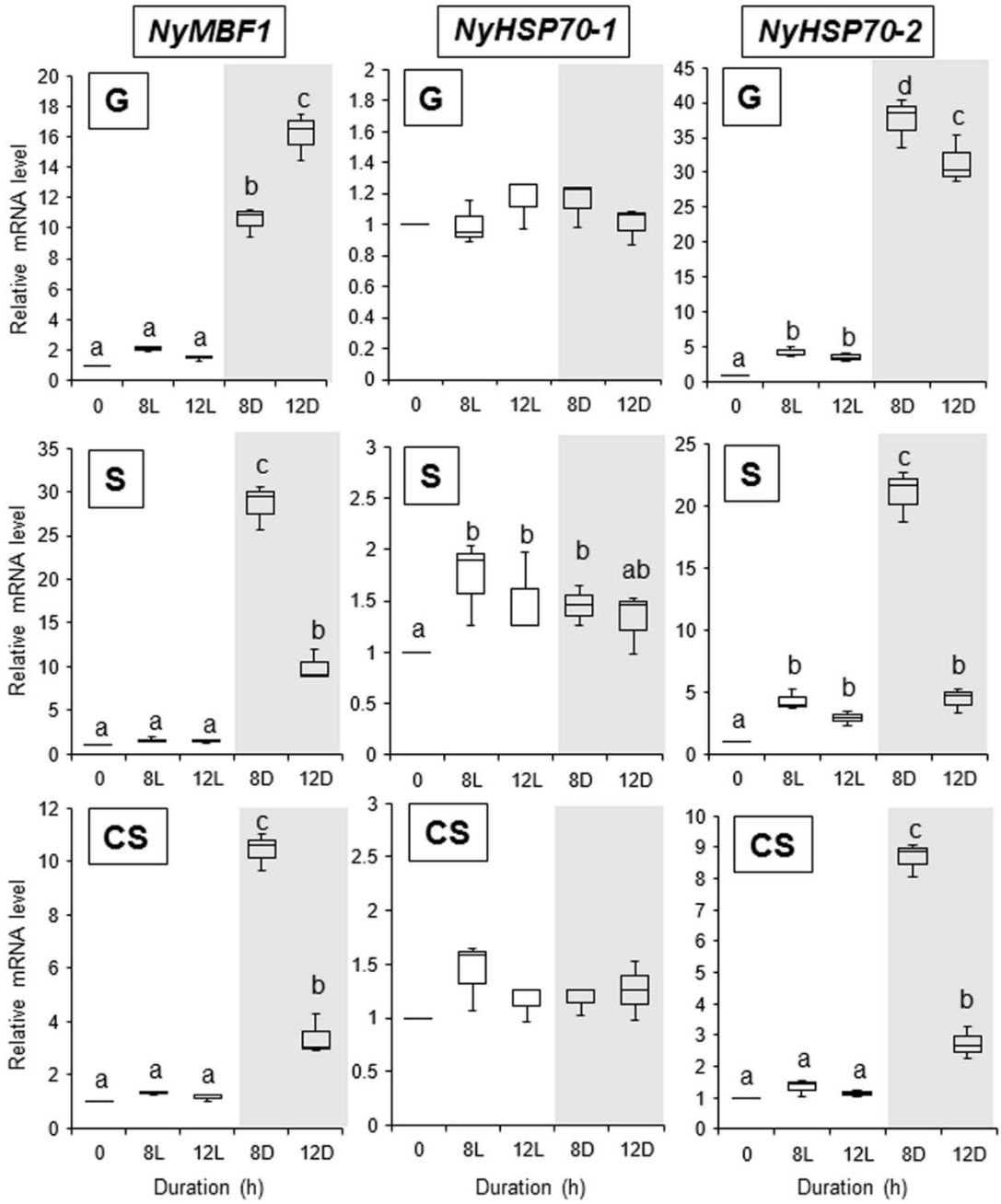
NyMBF1
NyHSP70-1
NyHSP70-2
G
S
CS
Relative mRNA level
Duration (h)
0
8L
12L
8D
12D

Figure 11

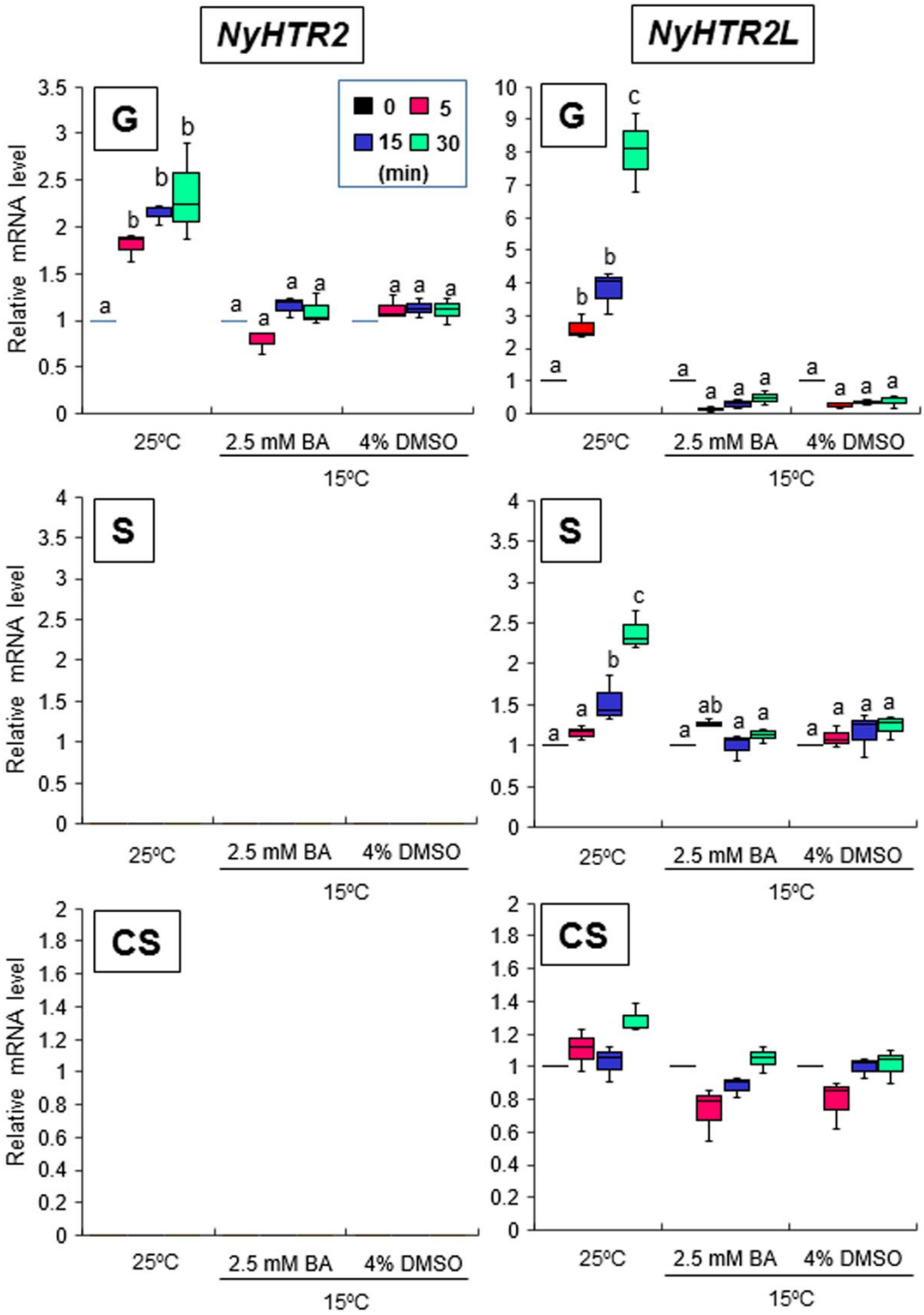
NyHTR2
NyHTR2L
G
S
CS
0
5
15
30
(min)
Relative mRNA level
25ºC
2.5 mM BA
4% DMSO
15ºC

Figure 12

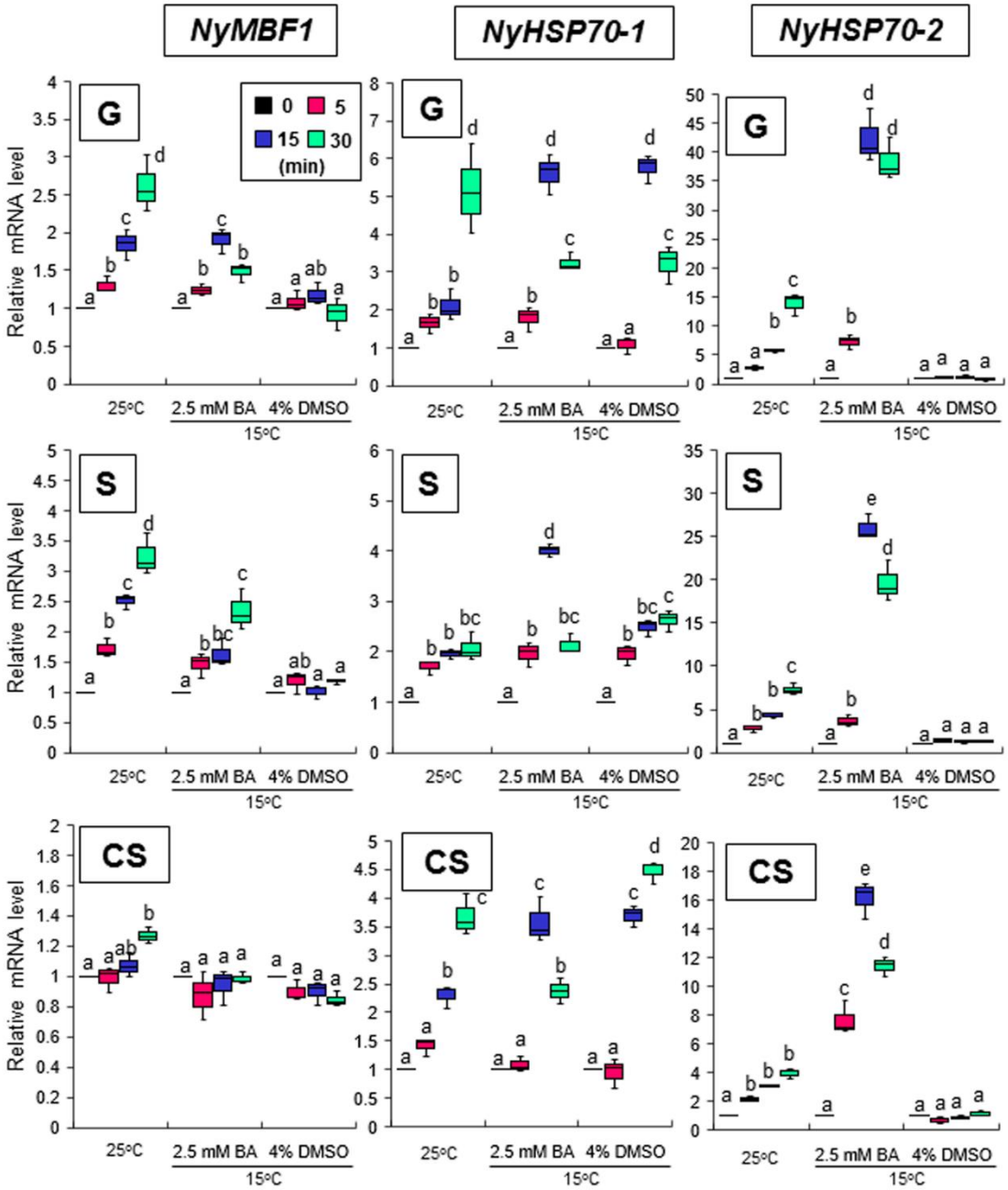
NyMBF1
NyHSP70-1
NyHSP70-2
G
S
CS
0
5
15
30
(min)
Relative mRNA level
25°C
2.5 mM BA
4% DMSO
15°C

Figure 13

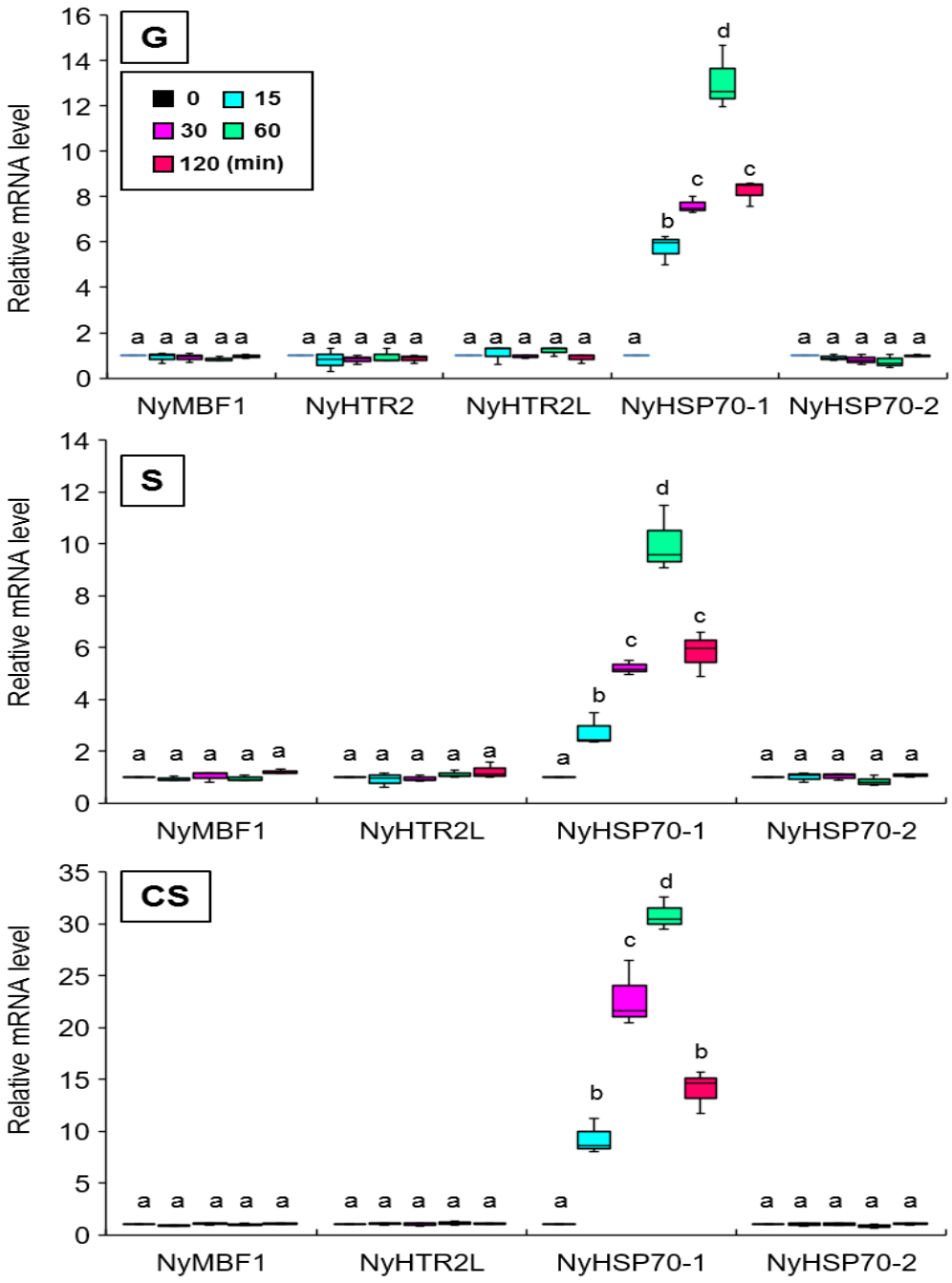
G
0
15
30
60
120 (min)
Relative mRNA level
NyMBF1
NyHTR2
NyHTR2L
NyHSP70-1
NyHSP70-2
S
CS

Figure 14

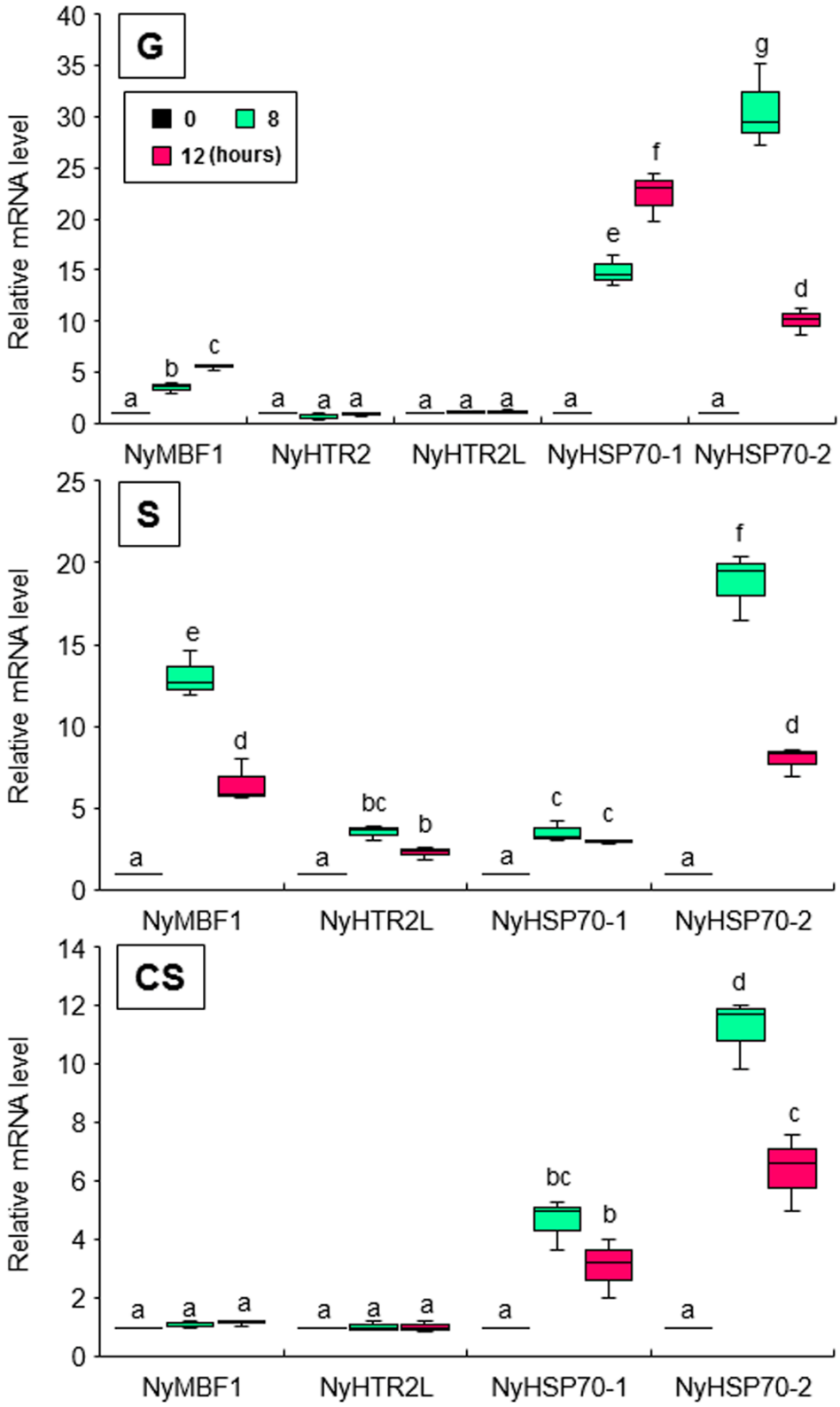
G
0
8
12 (hours)
Relative mRNA level
NyMBF1
NyHTR2
NyHTR2L
NyHSP70-1
NyHSP70-2
S
CS

Figure 15

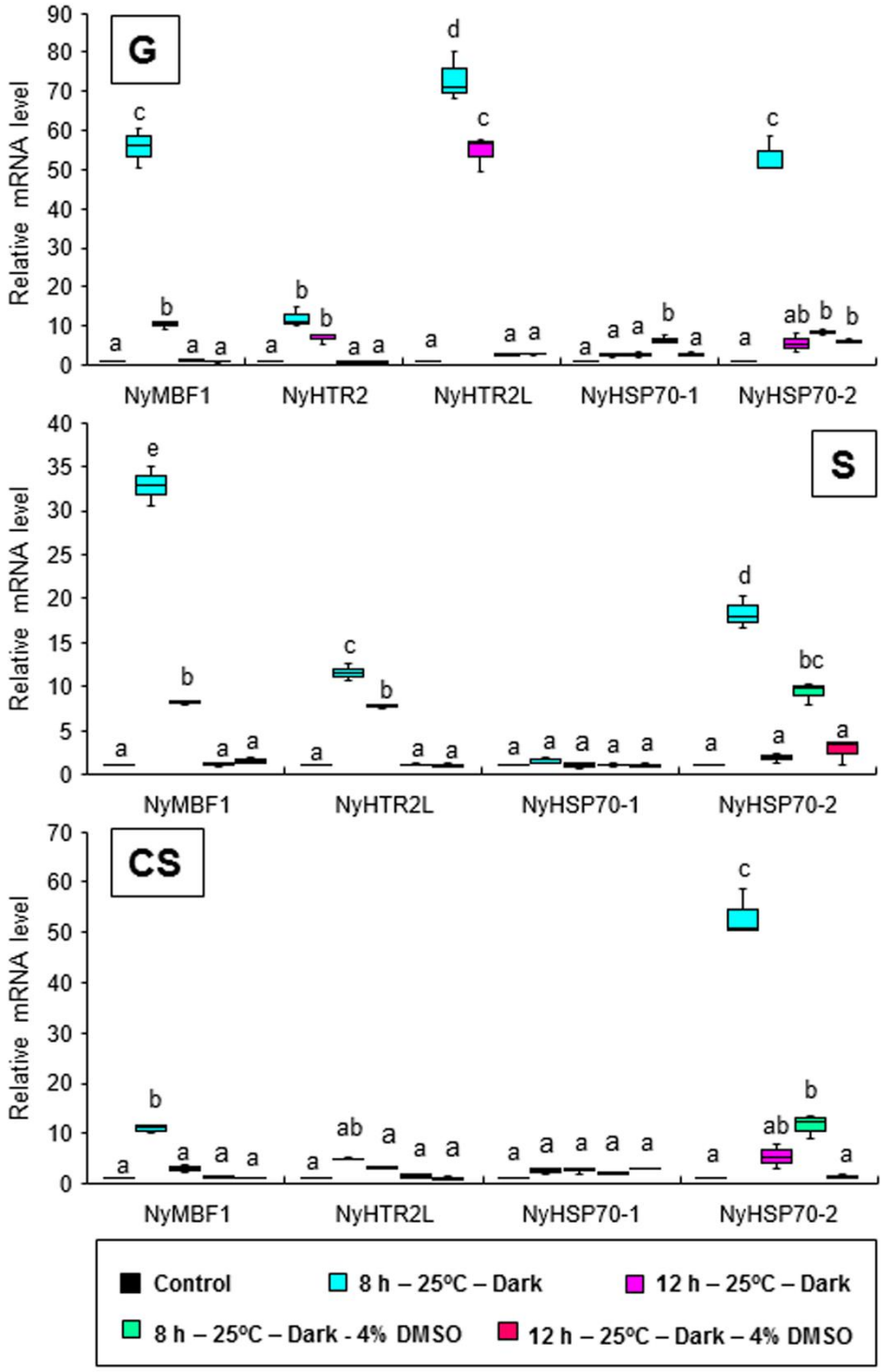
G
S
CS
Relative mRNA level
NyMBF1
NyHTR2
NyHTR2L
NyHSP70-1
NyHSP70-2
Control
8 h – 25ºC – Dark
12 h – 25ºC – Dark
8 h – 25ºC – Dark - 4% DMSO
12 h – 25ºC – Dark – 4% DMSO

Figure 16